JUL 1 5 1982

830-H-15 NAS 1.60:2030

NASA
Technical
Paper
2030

June 1982

COMPLETED
58

Computer Program for Calculating Full Potential Transonic, Quasi-Three-Dimensional Flow Through a Rotating Turbomachinery Blade Row

Charles A. Farrell

ORIGINAL

NASA

NASA Technical Paper 2030

1982

Computer Program for Calculating Full Potential Transonic, Quasi-Three-Dimensional Flow Through a Rotating Turbomachinery Blade Row

Charles A. Farrell
Lewis Research Center
Cleveland, Ohio

NASA
National Aeronautics and Space Administration

Scientific and Technical Information Branch

I

BEST DOCUMENT AVAILABLE

SUMMARY

A fast, reliable computer code is described for calculating the flow field about a cascade of arbitrary two-dimensional airfoils. The method approximates the three-dimensional flow in a turbomachinery blade row by correcting for stream-tube convergence and radius change in the throughflow direction. A fully conservative solution of the full potential equation is combined with the finite volume technique on a body-fitted periodic mesh, with an artificial density imposed in the transonic region to insure stability and the capture of shock waves. The instructions required to set up and use the code are included in this report. The name of the code is QSONIC. A numerical example is also given to illustrate the output of the program.

INTRODUCTION

In the area of internal flows the need to design lighter, more efficient turbomachine components has led to the consideration of machines with fewer stages, each with blades capable of higher speeds and higher loading. As speeds increase, the numerical problems inherent in the transonic regime have to be resolved. These include the calculation of imbedded shock discontinuities and the dual nature of the governing equations, which are elliptic in the subcritical flow regions but become hyperbolic for supersonic zones.

The present analysis combines some of the most promising transonic analysis techniques to calculate the flow field surrounding the cascade of airfoils. The full potential equation in conservative form is discretized at each point on a body-fitted period mesh, and a mass balance is calculated through the finite volume surrounding the point. Each local volume is corrected in the third dimension for any change in stream-tube thickness along the stream tube. The nonlinear equations for all volumes are of mixed type (elliptic or hyperbolic) depending on the local Mach number. The final result is a block-tridiagonal matrix formulation involving potential corrections at each grid point as the unknowns. The residual of each equation is equal to the net mass flux through a volume. The resulting system of equations is solved along each grid line by an SLOR procedure. At points where the Mach number exceeds unity, the density at the forward (sweeping) edge of the volume is replaced by an artificial density (ref. 1).

The capabilities of this FORTRAN program, beyond those of previous cascade analysis methods (ref. 2), include the ability to calculate through weak shocks (peak relative Mach number less than 1.4) and completely around both leading- and trailing-edge regions of a blade. The blade shapes in the leading- and trailing-edge regions are not restricted to circular arcs.

The flow field to be calculated can be axial, radial, or mixed and can be rotating or stationary. The geometry of the stream surface can be a two-dimensional planar cascade or axisymmetric with varying channel thickness and radial position. There are, however, several situations that cause unsatisfactory results because of the inviscid flow assumptions. Sharp leading edges at high incidence and high-Mach-number turbine blade trailing edges with substantial deviation will both cause large velocity peaks on the blade as the inviscid flow tries to negotiate the large angle from stagnation point to suction surface. In addition, if the passage is nearly choked, the code may have difficulty converging.

BEST DOCUMENT AVAILABLE

More details on the methods used by the code for grid generation are discussed in reference 3. In the following sections an overview of the program's capabilities is given, and an outline of the solution procedure is presented. A list of the necessary input, an interpretation of the output, and the basic flow logic of the code are given. Sufficient information is presented to allow a user to make use of the program. A detailed test case is also included for ease of verification.

PROGRAM DEFINITION

The QSONIC code was developed to obtain the transonic potential flow distribution on a blade-to-blade stream surface of a stationary or rotating turbomachine blade row.

Capabilities

The following assumptions were made in developing the analysis and the code:

(1) The flow is inviscid and adiabatic.
(2) The flow relative to the blade is steady.
(3) The fluid is a perfect gas with constant specific heat.
(4) The flow is isentropic and any discontinuities (shocks) are weak enough to be approximated as isentropic jumps.
(5) There is no velocity component normal to the stream surface (fig. 1). Flow is restricted to the two components within the stream surface: the streamwise direction (vector combination of axial and radial), and the tangential direction.
(6) The flow relative to a frame fixed in space (absolute velocity) is completely irrotational, and the flow relative to the blade can be represented as the vector addition of this absolute flow field minus the wheel speed in the tangential direction.

Assumption (6) is sufficient to allow the absolute velocity to be represented as a gradient of a potential field.

The flow field to be calculated can be axial, radial, or mixed. The compressor or turbine blade row can be fixed or rotating. As a result of assumption (4) the peak local relative Mach number should be 1.4 or less. The geometry of the stream surface can be a two-dimensional planar cascade or an axisymmetric configuration whose stream-sheet thickness and radius vary with distance along the stream surface. The extent of this surface that corresponds to one blade passage, with the blade in the center (see upper portion of fig. 1), is mapped into a rectangle for numerical simplicity by one of the two mesh generators (ref. 3) available in QSONIC.

Figure 2 gives major features of the solution process, including grid generation and refinement. There are essentially two modes in which the program can be operated: (1) One grid generation and a flow solution can be combined in a single execution. (2) A separate run is first made to generate and store a grid, and then the flow solver is used sequentially on several different meshes that are based on the stored grid (mesh refinement). Mesh refinement normally gives about a 30 percent gain in convergence speed over what can be attained by using the finest (stored) grid exclusively to meet a given convergence criterion.

BEST DOCUMENT AVAILABLE

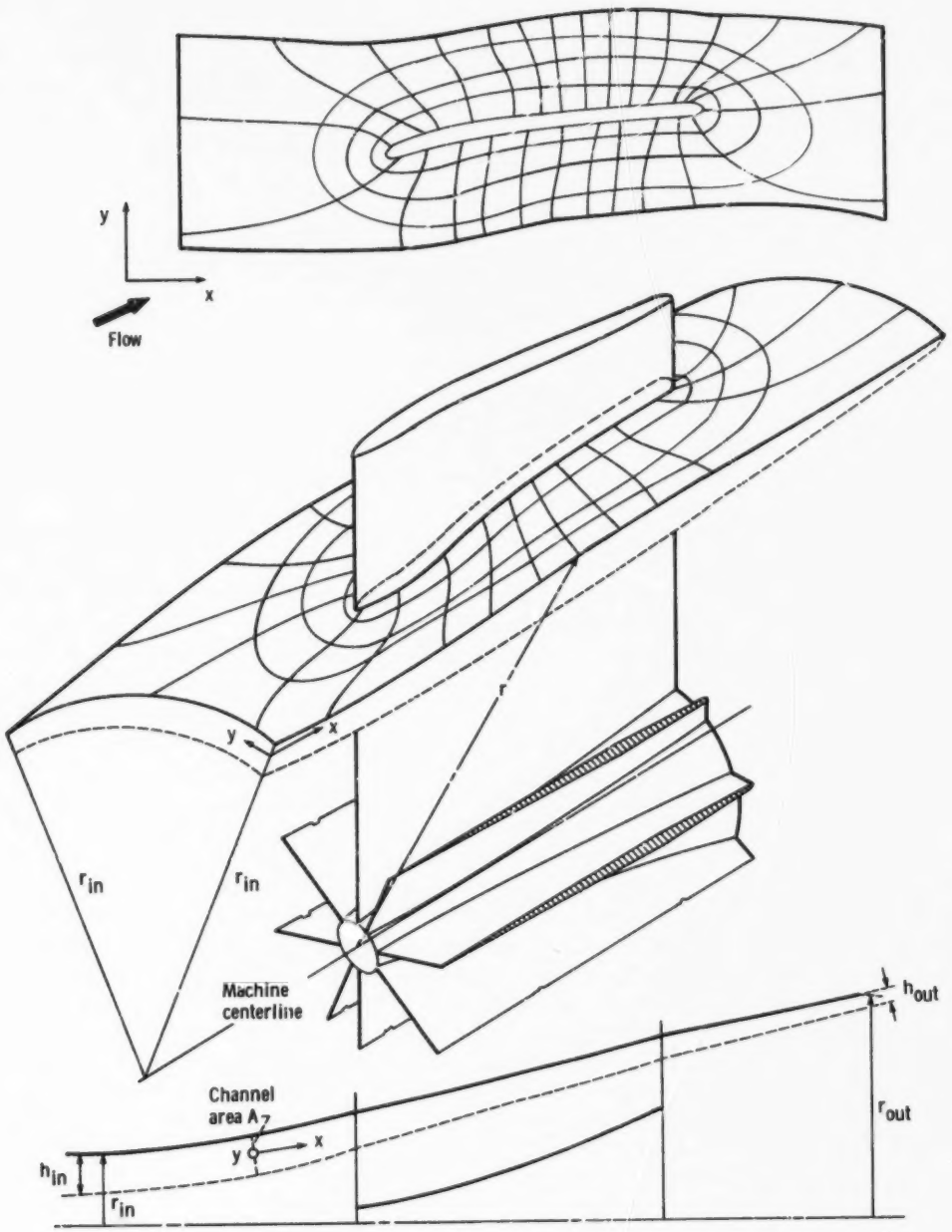

Figure 1. - Schematic of stream-channel surface.

BEST DOCUMENT AVAILABLE

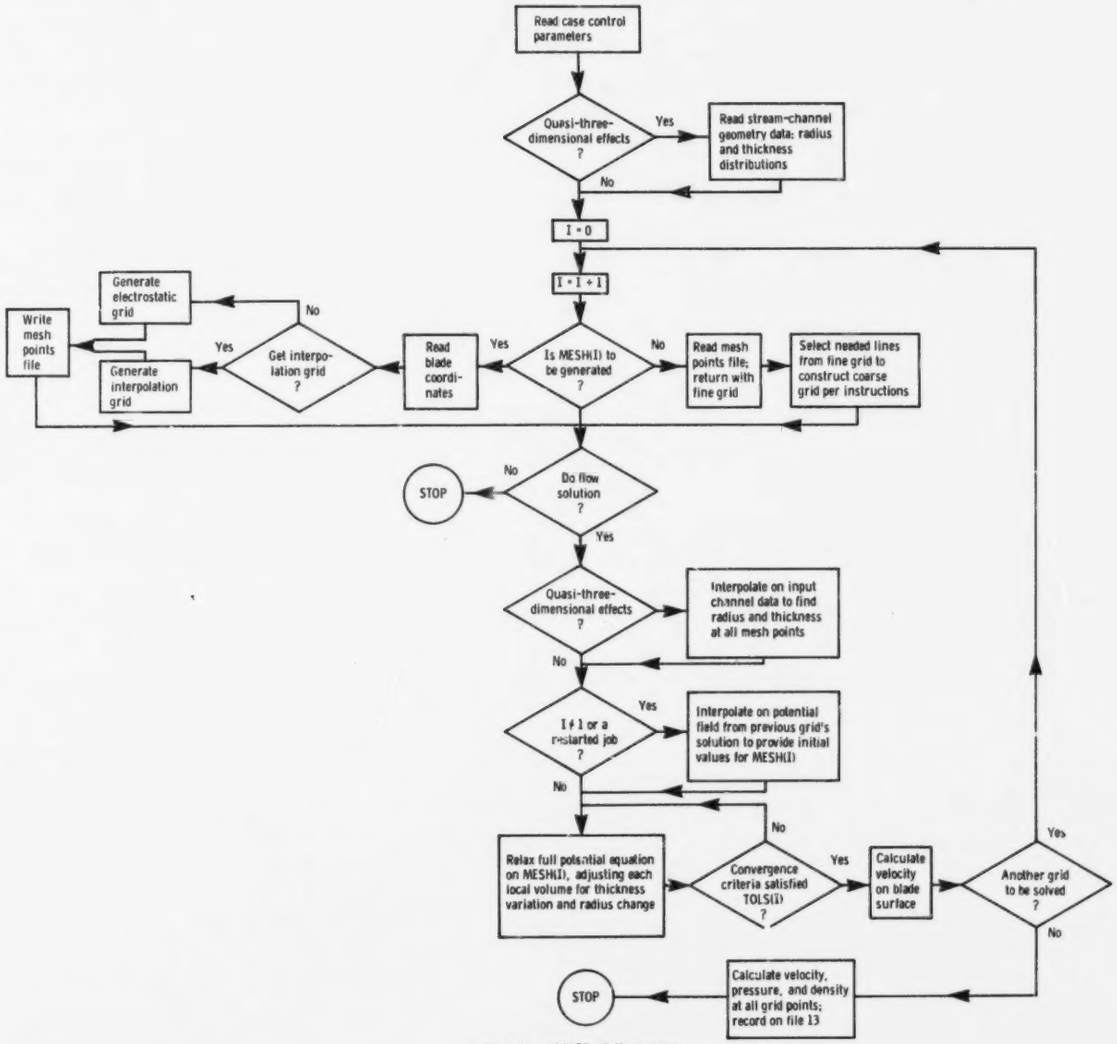
Read case control parameters
Quasi-three-dimensional effects ?
Yes
Read stream-channel geometry data: radius and thickness distributions
No
I = 0
I = I + 1
Generate electrostatic grid
No
Write mesh points file
Yes
Get interpolation grid ?
Generate interpolation grid
Read blade coordinates
Yes
Is MESH(I) to be generated ?
No
Read mesh points file; return with fine grid
Select needed lines from fine grid to construct coarse grid per instructions
STOP
No
Do flow solution ?
Yes
Quasi-three-dimensional effects ?
Interpolate on input channel data to find radius and thickness at all mesh points
No
I ≠ 1 or a restarted job ?
Yes
Interpolate on potential field from previous grid's solution to provide initial values for MESH(I)
No
Relax full potential equation on MESH(I), adjusting each local volume for thickness variation and radius change
No
Convergence criteria satisfied TOLS(I) ?
Yes
Calculate velocity on blade surface
Another grid to be solved ?
Yes
No
STOP
Calculate velocity, pressure, and density at all grid points; record on file 13

Figure 2. - QSONIC solution process.

BEST DOCUMENT AVAILABLE

Limitations

Flow Solution Method

Although the program will perform well for a wide variety of turbine and compressor blading and flow conditions, there are several situations that cause unsatisfactory results because of the potential flow assumptions. Since the flow is to be inviscid and irrotational, sharp leading edges at high incidence (more than a few degrees) will cause large velocity peaks on the blade surface as the inviscid flow tries to negotiate the large angle turn from stagnation point to suction surface. Such peaks should be discounted. The remainder of the flow field will still be reliable since these peaks seldom poison more than a few grid points in their vicinity. This situation arises most often with thin-blade compressor geometries, where the adverse flow gradient on the suction surfaces tends to discourage the velocity fluctuations from propagating very far or reflecting off the downstream boundaries.

The conditions are not so favorable at the trailing edge of high-Mach-number turbine blades, where a more serious problem can arise. Here the flow is at its highest velocity, the blade has its minimum thickness, proximity to neighboring blades is enhanced (in the area of the passage throat), and the flow gradient is favorable for carrying errors and velocity peaks toward the downstream boundary and further reflection. Velocity spikes that arise here can be very severe, propagating across the narrow passage and eventually choking or poisoning the entire region. The safest method for using the code on geometries such as this is to approach the actual conditions slowly. Begin with a coarse grid (no more than 14 cells across the passage) and slowly increase the upstream Mach number or vary the downstream flow angle (away from minimum deviation) in the neighborhood of the desired values. If more than three points on the blade surface exceed Mach 2, the solution is not reliable.

A third and final area of difficulty for the code is choking flow since the mass flow is determined by the upstream boundary conditions and global continuity is assumed. But whether a particular shape of passage is choked or not can only be determined by executing the code. The program may run to completion for nearly choked passages (maximum mass flow), but the solution would be unreliable if there were an area of Mach 1.1 extending more than halfway across the passage.

Grid Generation Method

The generator referred to as the interpolation scheme (ref. 3) is best applied to compressor or turbine blading of low to moderate camber and thickness. This mesh generation scheme has no problem with large stagger angles ($\approx 75^\circ$) nor with high solidities. Cases with solidities of 1.45 have been attempted with good results. However, if the turning angle or thickness of the blade is large, while at the same time stagger and solidity are near the limits mentioned above (i.e., stagger plus turning $\approx 124^\circ$), the grid lines may become crowded on the suction surface. This is common for turbine blade geometries. The interpolation scheme does not perform well for blades with very small leading- or trailing-edge radii (knife edges). It does have the advantages of allowing some control over placement of grid lines by concentrating them near the blade surface or in the trailing-edge region and also of blade coordinate smoothing.

BEST DOCUMENT AVAILABLE

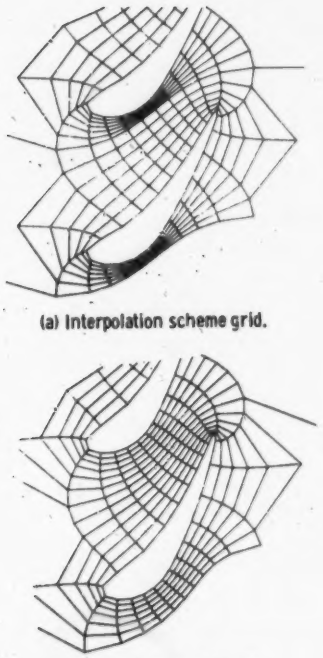

(a) Interpolation scheme grid.

(b) Electrostatic analog grid.

Figure 3. - Coarse mesh for turbine cascade.

The electrostatic analog scheme (ref. 3) was designed to handle thick turbine blades of high camber, thickness, and solidity, so it is general enough to handle any possible blade geometry, including knife-edge profiles. The disadvantages are the lack of control over grid line concentration and no smoothing. Figure 3 shows results of the two generators for the same turbine cascade. Both grids shown were successful in subsequent flow solution runs.

Program Operations

The FORTRAN code for QSONIC was developed on an IBM 3033/370. The accuracy for the present version of QSONIC is limited to single precision (for this machine, seven decimal digits). The program requires 58 000 words or core storage to execute a separate geometry generation run with the interpolation scheme. This rises to 63 000 words for an electrostatic analog grid generation. An execution that combines either of the grid generators with a flow solution requires 210 000 words, provided that the common blocks (ENTIRE, GEOM, and GEOM2) containing the mesh coordinates and parameters are loaded separately and the grid generator codes are overlayed with the flow solver module. If the entire code is loaded simultaneously, the maximum core size needed is 240 000 words. If common block HIBALL is eliminated (used for metric storage to avoid recalculation), this reduces to 90 000 words. In all applications the BLOCK DATA module should be the first one loaded.

BEST DOCUMENT AVAILABLE

SOLUTION METHOD

Governing Equations

The flow field relative to a frame fixed in space (the absolute system) is assumed to be irrotational, isentropic, and inviscid. Thus the continuity equation

$$\frac{\partial \rho}{\partial t} + \overline{\nabla} \cdot (\rho \overline{V}) = 0 \tag{1}$$

where $\overline{V}$ is the absolute velocity, can be rewritten with $\overline{V}$ being the gradient of a potential field

$$\left.\begin{aligned} &\overline{V} = \overline{\nabla}\varphi \\ &\text{and} \\ &\frac{\partial \rho}{\partial t} + \overline{\nabla} \cdot (\rho \overline{\nabla}\varphi) = 0 \end{aligned}\right\} \tag{2}$$

But this field is unsteady because of the passing blade. If we assume that the coordinate system is fixed to the blade, continuity takes the desired steady form

$$\left.\begin{aligned} &\overline{\nabla} \cdot (\rho \overline{W}) = 0 \\ &\text{where} \\ &\overline{W} = \overline{V} - \overline{\Omega} \times \overline{r} \end{aligned}\right\} \tag{3}$$

which is just the absolute velocity minus the wheel speed in the tangential direction.

It is required that equation (3) hold at each point in the flow field. As suggested by several others (refs. 4 and 5), equation (3) is integrated over the element of volume at each point. Making use of the divergence theorem gives

$$\int_V \overline{\nabla} \cdot (\rho \overline{W})\, d\mathcal{V} = \int_{A_E} \rho \hat{n} \cdot \overline{W}\, dA_E = 0 \tag{4}$$

where $\hat{n}$ is the outward normal to the area element dA, $\mathcal{V}$ the element volume, and A_E the surface area of the element.

Approximating the integral as the sum over the four element faces shown in figure 4 gives

BEST DOCUMENT AVAILABLE

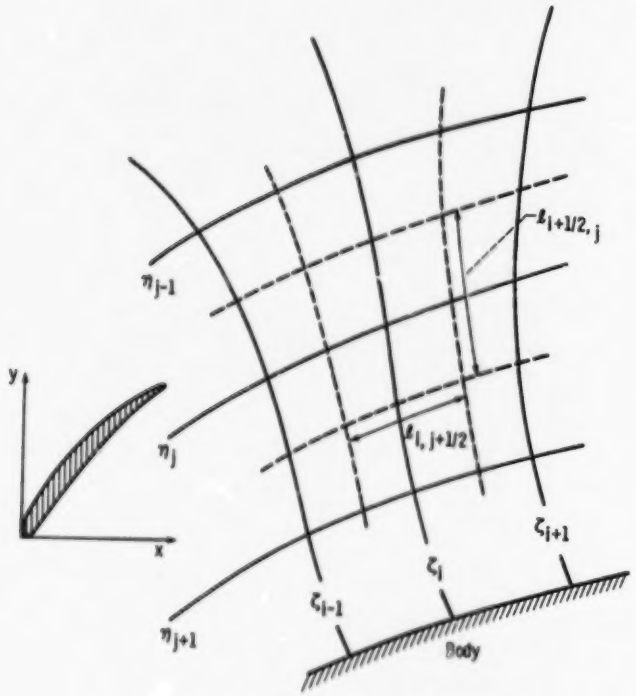

Figure 4. - Finite volume element in physical space.

$$\int_{A_E} \rho \bar{n} \cdot W \, dA_E \doteq \sum \rho \bar{W} \cdot \hat{n} \, \Delta A_E = 0 \tag{5}$$

Defining

$$R^K = \sum {}^{\rho^k \bar{W}^k} \cdot \hat{n} \, \Delta A_E \tag{5a}$$

as the net flow out of the element at iteration K gives for convergence

$$R^{K+1} = R^K + \delta R^K = 0 \tag{6}$$

or

$$\delta R^K = -R^K \tag{6a}$$

BEST DOCUMENT AVAILABLE

If we differentiate equation (5a) to form δR^K, equation (6a) becomes

$$\delta R^K = \sum \left(\bar{W}^K \cdot \hat{n} \delta \rho^K \, \Delta A_E + \rho^K \hat{n} \cdot \delta \bar{W}^K \, \Delta A_E \right) = - \sum \rho^K \bar{W}^K \cdot \hat{n} \, \Delta A_E \tag{7}$$

But for isentropic flow

$$\frac{\rho^{\gamma-1}}{\rho_{in}^{\gamma-1}} = 1 + \frac{\gamma - 1}{2} M_{in}^2 \left\{ 1 - \frac{W^2}{W_{in}^2} + \frac{\Omega^2 r_{in}^2}{W_{in}^2} \left[\left(\frac{r}{r_{in}} \right)^2 - 1 \right] \right\} \tag{8}$$

and for this potential flow

$$\bar{W} = \bar{\nabla} \varphi - \bar{\Omega} \times \bar{r} \tag{9}$$

Then δR^K can be expressed as a function of the local geometry and the potential values for φ. From equation (8), since ρ is a function of W,

$$\delta \rho^K = \frac{\partial \rho}{\partial W} \delta W^K \tag{10}$$

From equation (9), after transformation to the computational (η,ζ) space, for $\delta \bar{W} = \delta u \hat{i} + \delta v \hat{j}$,

$$\delta u^K = \frac{\partial (\delta \varphi)^K}{\partial \eta} \frac{\partial \eta}{\partial x} + \frac{\partial (\delta \varphi)^K}{\partial \zeta} \frac{\partial \zeta}{\partial x} \tag{11}$$

and

$$\delta v^K = \frac{\partial (\delta \varphi)^K}{\partial \eta} \frac{\partial \eta}{\partial y} + \frac{\partial (\delta \varphi)^K}{\partial \zeta} \frac{\partial \zeta}{\partial y} \tag{12}$$

where

$$\delta \varphi^K = (\varphi^{K+1} - \varphi^K) \frac{1}{\omega} \tag{13}$$

is the unknown correction to the local potential field, and ω is an overrelaxation factor to accelerate convergence.

If we substitute equations (8), (10), (11), and (12) into equation (7) and recall that the area ΔA_E of each face of the element is just the product of its length ℓ and stream-channel thickness h, we obtain

BEST DOCUMENT AVAILABLE

$$\sum \left\{ \left[\left(u^K e_x + v^K e_y \right) \frac{\partial \rho^K}{\partial W} \frac{u^K}{W^K} + \rho^K e_x \right] \left(\frac{\partial (\delta\varphi)^K}{\partial \eta} \frac{\partial \eta}{\partial x} + \frac{\partial (\delta\varphi)^K}{\partial \zeta} \frac{\partial \zeta}{\partial x} \right) \right.$$

$$\left. + \left[\left(u^K e_x + v^K e_y \right) \frac{\partial \rho^K}{\partial W} \frac{v^K}{W^K} + \rho^K e_y \right] \left(\frac{\partial (\delta\varphi)^K}{\partial \eta} \frac{\partial \eta}{\partial y} + \frac{\partial (\delta\varphi)^K}{\partial \zeta} \frac{\partial \zeta}{\partial y} \right) \right\} \ell h$$

$$= - \sum \rho^K (u e_x + v e_y)^K \ell h \qquad (14)$$

where the normal vector to each face is

$$\hat{n} = e_x \hat{i} + e_y \hat{j} \qquad (15)$$

The right side of equation (14), $R_{i,j}$, is the residual net mass flow out of the finite volume surrounding the grid point (i,j). Each volume element is defined by the four surfaces parallel to and located halfway between neighboring grid lines, as shown in figure 4. Several schematic views of the quasi-three-dimensional stream surface are presented in figure 1. The thickness of the element (i.e., relative local stream-tube height) and its radial position are obtained from specified distributions. Height is set to unity for planar two-dimensional flow. Variations in the radius r of the stream tube are accounted for by scaling tangential $r\theta$ coordinates y with a ratio of the local radius r to a given upstream radius r_{LE}. Then over the area A_E defined by the four surfaces of the volume element,

$$R_{i,j} = \int_{A_E} \rho \overline{W} \, dA = \sum \left(\rho^K_{i\pm1/2,j} \overline{W}^K_{i\pm1/2,j} \ell_{i\pm1/2,j} h_{i\pm1/2,j} \right.$$

$$\left. + \rho^K_{i,j\pm1/2} \overline{W}^K_{i,j\pm1/2} \ell_{i,j\pm1/2} h_{i,j\pm1/2} \right) \qquad (16)$$

where h is the local stream-tube height normalized to unity far upstream. The velocities $\overline{W}$ are normal to the element boundaries and located at the boundaries. Velocity $\overline{W}$ and density ρ are calculated from values of potential at the previous iteration.

The summation shown on the left side of equation (14) proceeds in the same manner as that for R. Quantities are calculated at the center of each face (fig. 4), $(i, j + 1/2)$, $(i, j - 1/2)$, $(i + 1/2, j)$, $(i - 1/2, j)$, and finite differences are formed by using potential correction values at neighboring points. As an example,

BEST DOCUMENT AVAILABLE

$$\left.\frac{\partial(\delta\varphi)^K}{\partial\eta}\right|_{i,j+1/2} = \frac{\delta\varphi^K_{i,j+1} - \delta\varphi^K_{i,j}}{\eta_{j+1} - \eta_j} \tag{17}$$

and for cross terms

$$\left.\frac{\partial(\delta\varphi)^K}{\partial\zeta}\right|_{i,j+1/2} = 1/2\left(\frac{\delta\varphi^{K-1}_{i+1,j+1} - \delta\varphi^K_{i,j+1}}{\zeta_{i+1} - \zeta_i} + \frac{\delta\varphi^{K-1}_{i+1,j} - \delta\varphi^K_{i,j}}{\zeta_{i+1} - \zeta_i}\right) \tag{18}$$

If we make use of the relations and similar expressions for the other faces and isolate all unknown potential corrections on the left side, equation (14) can be expressed in the form

$$A_{i,j+1}\delta\varphi^K_{i,j+1} + A_{i,j}\delta\varphi^K_{i,j} + A_{i,j-1}\delta\varphi^K_{i,j-1} = \mathcal{R}^K_{i,j} \tag{19}$$

where

$$\mathcal{R}_{i,j} = -R_{i,j} + G\left(\varphi^K, \rho^K, \delta\varphi^K_{i-1}, \delta\varphi^{K-1}_{i+1}\right) \tag{20}$$

By writing equation (19) for each point on a grid line of constant ζ ($j = 1,J$), a tridiagonal matrix system is formed that is then solved by the standard Thomas algorithm (ref. 6) for the potential corrections $\delta\varphi^k$. New values of the field potential are obtained by using equation (13) after all lines are solved ($i = 1,I$).

The coefficients in equation (19) are

$$\left.\begin{aligned}
A_{i,j+1} &= \frac{\left[\varepsilon h\rho^K\left(\frac{\partial\eta}{\partial x}e_x + \frac{\partial\eta}{\partial y}e_y\right)\right]_{i,j+1/2}}{\eta_{j+1} - \eta_j} \\
A_{i,j-1} &= \frac{\left[\varepsilon h\rho^K\left(\frac{\partial\eta}{\partial x}e_x + \frac{\partial\eta}{\partial y}e_y\right)\right]_{i,j-1/2}}{\eta_{j-1} - \eta_j} \\
A_{i,j} &= -A_{i,j+1} - A_{i,j-1} + \frac{\left[\varepsilon h\rho^K\left(\frac{\partial\zeta}{\partial x}e_x + \frac{\partial\zeta}{\partial y}e_y\right)\right]_{i+1/2,j}}{\zeta_{i+1} - \zeta_i} \\
&\quad + \frac{\left[\varepsilon h\rho^K\left(\frac{\partial\zeta}{\partial x}e_x + \frac{\partial\zeta}{\partial y}e_y\right)\right]_{i-1/2,j}}{\zeta_{i-1} - \zeta_i}
\end{aligned}\right\} \tag{21}$$

BEST DOCUMENT AVAILABLE

Sweep Strategy

The grid lines are solved in order, beginning with the line that goes to downstream infinity and then proceeding clockwise around the blade shape. This order results in a solution that sweeps against the flow direction on the bottom surface of a blade. It became evident, when symmetric supersonic flows were successfully solved, that direction of sweep relative to the flow is not critical. The apparent reason is that additional damping is applied by the elliptic-like nature of the artificial density when it is used in combination with the sweep strategy. More details on the effect are given in the next section.

Artificial Density

In equation (7) there is no explicit artificial viscosity term necessary for stability in supercritical flow regions and for smearing shock jumps. As suggested by Hafez et al. (ref. 1), an implicit viscosity term is incorporated in the density. This modified density is used instead of the physical density in equation (7). Subsequent numerical experiments indicated that modifying the densities on the left side of equation (7) at each iteration level was not necessary. Thus, to speed the calculation, there is a parameter (IT) that controls how often to update the densities. The form of the artificial viscosity modification is (ref. 1)

$$\tilde{\rho} = \rho - \mu \rho_S \, \Delta S \tag{22}$$

where μ is the switching function to eliminate the density modification in subsonic regions ($M < 1$)

$$\mu = \max\left(0, \; 1 - \frac{1}{M^2}\right) \tag{23}$$

where M is the Mach number relative to the moving blade row and $\rho_S \, \Delta S$ is the total differential component of the density in the flow direction S defined by the contravariant velocity components a and b. Then

$$\mu \rho_S \, \Delta S = \mu_a \frac{a}{q} \rho_\eta \, \Delta\eta + \mu_b \frac{b}{q} \rho_\zeta \, \Delta\zeta \tag{24}$$

where

$$q = \sqrt{u^2 + v^2}$$

and

$$\rho_\eta = \frac{\partial \rho}{\partial \eta}, \qquad \rho_\zeta = \frac{\partial \rho}{\partial \zeta}$$

BEST DOCUMENT AVAILABLE

The switching function was split into two terms so that the effect of each component of the density change could be even more efficiently gaged in areas of high flow gradient. In addition, an upwind-averaged Mach number was used:

$$\left.\begin{aligned} \mu_a &= \max\left(0,\ 1 - \frac{1}{M^2_{av_a}}\right) \\ &\text{where} \\ M_{av_a} &= \tfrac{1}{2}\left(M_{i+1/2,j} + M_{i+1/2,j\pm1}\right) \\ \mu_b &= \max\left(0,\ 1 - \frac{1}{M^2_{av_b}}\right) \\ &\text{where} \\ M_{av_b} &= \tfrac{1}{2}\left(M_{i+1/2,j} + M_{i+1/2\pm1,j}\right) \end{aligned}\right\} \qquad (25)$$

Similarly, upwind differencing is used for approximating ρ_ζ and ρ_η: The physical densities used to calculate ρ_ζ and ρ_η are updated as each line is reached. Implicit in this arrangement is the creation of a timelike cross derivative of density ρ_{st} when sweeping against the flow direction. This cross derivative is created because the density at the current line has been calculated by using the values of potential and velocity at the latest iteration (i.e., artificial time step), but the values at the next upstream line, where the upwind differences are formed, remain at the previous time step until they in turn are solved. However, when sweeping with the flow, the upstream line from which the density gradients are formed has already been solved and updated. Thus this additional damping due to the time lag of densities is not present when solving with the flow, and the artificial compressibility reduces to the original space lag only.

Boundary Conditions

The boundary conditions applied to the solution system include a specified upstream axial mass flow, in the form of an oncoming Mach number, plus incidence and stagger angles. Using global continuity,

$$\rho_{out} u_{out} A_{out} = \rho_{in} u_{in} A_{in} \qquad (26)$$

BEST DOCUMENT AVAILABLE

where A is the flow area normal to the velocity u (fig. 1).

The specified flow angle at the downstream boundary, together with a simple iteration procedure on the isentropic density ratio, gives the downstream Mach number boundary condition. For a stagger angle λ and upstream relative angle of attack β_{in}, equation (26) can be expressed as

$$M_{out}\left(\frac{1}{1+\frac{\gamma-1}{2}M_{out}^2}\right)^{\frac{\gamma+1}{2(\gamma-1)}} = F(M_{out}) = \frac{A_{in}}{A_{out}}\frac{\cos\alpha_{in}}{\cos\alpha_{out}}M_{in}$$

$$\times\left\{\frac{1}{1+\frac{\gamma-1}{2}M_{in}^2\left[1+\frac{\Omega^2 r_{in}^2}{W_{in}^2}\left(\frac{r_{out}^2}{r_{in}^2}-1\right)\right]}\right\}^{\frac{\gamma+1}{2(\gamma-1)}} \tag{27}$$

where $\alpha = \beta + \lambda$, Ω is the rotational speed, and r is the radius of the stream channel. Using a straightforward Newton iteration on equation (27) yields M_{out}. From this the relative speed ratio is available as

$$\frac{q_{out}}{q_{in}} = \frac{M_{out}a_{out}}{M_{in}a_{in}} = \left[\frac{1+\frac{\Omega^2 r_{in}^2}{W_{in}^2}\left(\frac{r_{out}^2}{r_{in}^2}-1\right)+\frac{2}{\gamma-1}M_{in}^{-2}}{1+\frac{2}{\gamma-1}M_{out}^{-2}}\right]^{1/2} \tag{28}$$

Through trigonometric manipulation of the upstream and downstream velocity triangles, by using the input values of stagger, relative incidence, and rotational speed, the absolute flow angles α_a are obtained. The values of the velocities at volume elements that touch the far-field boundary are then calculated by using equation(26) and assuming constant angular momentum in the far field. Thus

$$\rho uA = \rho_{in}u_{in}A_{in} \tag{29}$$

with

$$rv = \frac{\partial\varphi}{\partial\theta} = \text{Constant} \tag{30}$$

Since density is a function of velocity, equation (29) can be rearranged for a Newton iteration procedure to obtain u at each border element point.

BEST DOCUMENT AVAILABLE

$$f(u) = u - \frac{\rho_{in} u_{in} A_{in}}{\rho(u,v) A} \to 0 \tag{31}$$

Periodicity is maintained in the tangential (y) direction by enforcing the relation

$$\varphi(x, y + s) = \varphi(x,y) + C \tag{32}$$

where s is the blade spacing and

$$C = \oint_{(x,y)}^{(x,y+s)} V \cdot d\hat{\ell} = V_{in} s_{in} \tag{33}$$

On the grid line defining the body, a standard zero-normal flow condition is imposed.

$$(\overline{\nabla}\varphi - \Omega r\hat{j}) \cdot \hat{n} = 0 \tag{34}$$

DESCRIPTION OF SUBROUTINES

Figure 5 illustrates the calling relationships between the main module and its subroutines.

Executive

MAIN QSONIC	Reads case control namelist for each job. Calls geometry setup, stream-channel data supplier, and flow solver for each of several grids requested (mesh refinement). References final output generator after last mesh is solved.
BLOCK DATA	Initializes all data values for variables that are in common blocks. Nonexecutable.

Geometry Generation

WRAPUP	Sets up geometry. For a new blade, reads bulk namelist of body coordinates, normalizes all dimensions to aerodynamic chord, and calls the mesh generator that was requested. For geometries already developed, reads file containing grid of maximum fineness and selects grid lines at proper intervals to create the coarser grid requested. Rearranges data arrays so that (1) the first row of each matrix contains the line going to downstream infinity, (2) the aerodynamic chord lies along the x axis, and (3) the origin is at midchord.
PJGRID	Generates a mesh by using the electrostatic analog method (ref. 3).

BEST DOCUMENT AVAILABLE

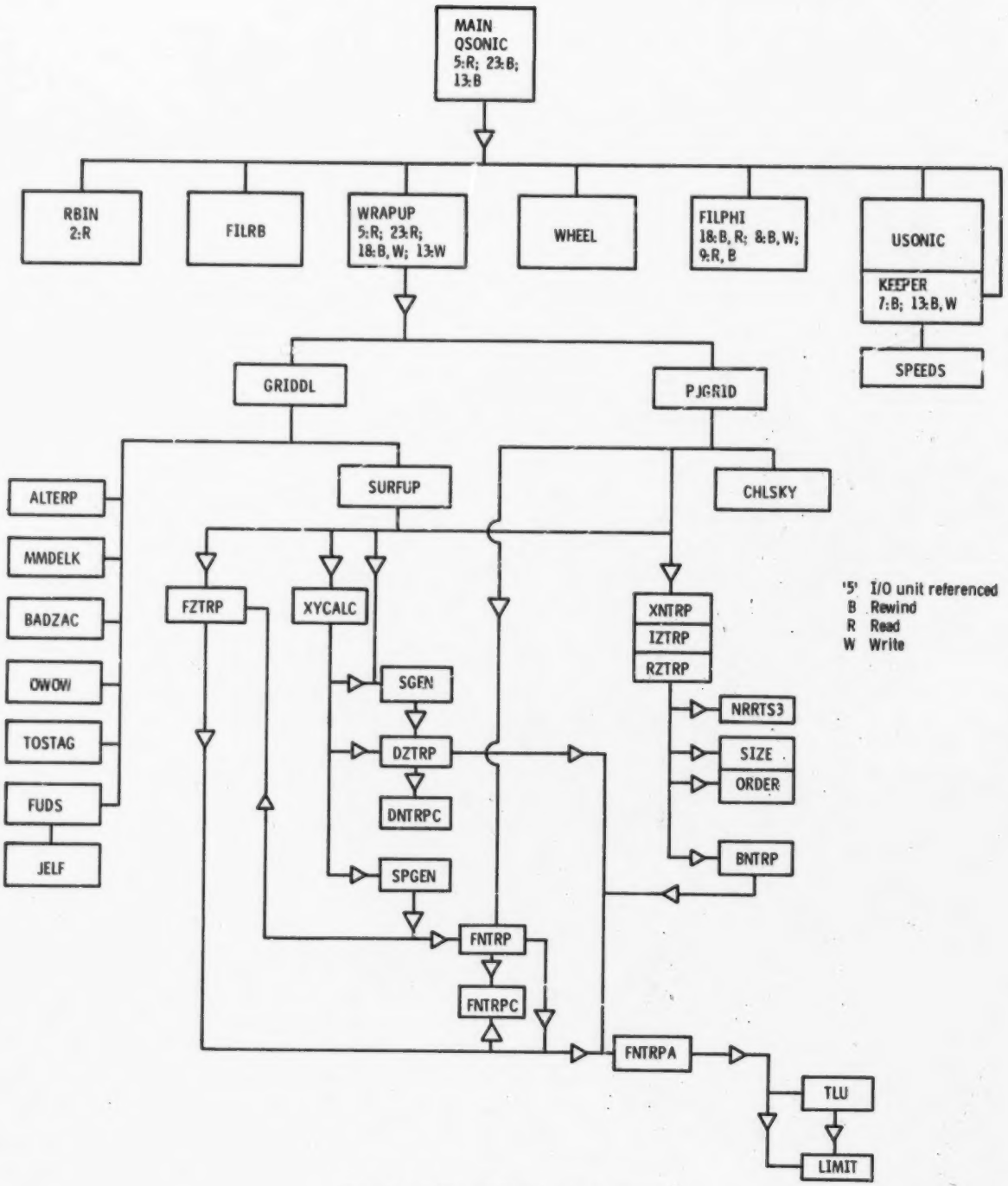

Figure 5. - Calling relationship between modules.

BEST DOCUMENT AVAILABLE

CHLSKY	Uses Cholesky's method to solve a linear system of equations (ref. 7).
GRIDDL	Generates a mesh by using the interpolation scheme: (1) Performs analytical transformation steps (2) Calls module to incorporate blade shape within flat-plate grid
SURFUP	Stretches the coordinates of the flat-plate mesh so that the desired blade surface becomes the innermost closed curve (grid boundary).
TOSTAG	Transforms the flat-plate cascade at zero stagger into the circle plane. Rotates the circle to the desired stagger and inverts the transformation back to the physical plane.
ALTERP	Interpolates on tabular values of solidity and stagger for the location of the positive and negative infinity points in the circle plane.
FUDS	Calculates one of the functions needed (defined as T in eq. (1), ref. 3) for transformation of the flat-plate cascade into the rectangle in computational space. Calls routine to calculate Jacobian elliptic functions.
OWOW	Calculates the function defined as Ω in equation (1), reference 3, needed for the transformation to a rectangle.
BADZAC	Calculates the function defined as Γ in equation (1), reference 3.
JELF	Calculations Jacobian elliptic functions SN, CN, and DN.
MMDELK (IOPT,ARG,IER)	Computes double-precision value of complete elliptic integral of the first kind, for $d\varphi/\mathrm{SQRT}$. $(1. - \mathrm{ARG} \cdot \mathrm{SIN}^2\varphi)$. IOPT = 1, $0 \leq \mathrm{ARG} < 1$.
WHEEL	Rotates x,y coordinates to the stagger angle.

Interpolation and Smoothing

XYCALC	Smooths the curve defined with the input points by generating additional points along the curve. The input is used to develop double three-point interpolating polynomials in successive regions along curve. Polynomials are then used to suggest points that can be tested against the spacing criteria as defined in the SPGEN listing.

BEST DOCUMENT AVAILABLE

SGEN	Computes line integral of the distance along the curve defined by the array of input point pairs.
SPGEN	Generates a table of points along the line integral as widely spaced as possible (see SPGEN listing for details).
LIMIT (I,J,K)	Limits J between I and K, i.e., if J < I, J = I; if J > K, J = K.
DZTRP	Evaluates complex derivative for three-point interpolation.
FNTRP	Evaluates real function for three-point interpolation.
FNTRPA	Evaluates first coefficients for three-point interpolation.
DNTRPC	Evaluates final coefficients of derivatives for three-point interpolation.
FNTRPC	Evaluates final function coefficients for three-point interpolation.
TLU (TABLE, ARG,N,I)	Table lookup of I, such that TABLE(I) < ARG < TABLE (I + 1)
FZTRP (S,F,A,N)	Interpolates on line integral array S, corresponding to point pairs in F, to find A on S. Returns matching point of F.
XNTRP(S,F,FO,N, ANS), with entry points IZTRP(S,F, FO,N,ANS) and RZTRP(S,F,FO,N,ANS)	Inverse of function FZTRP, which interpolates on complex array F to find the imaginary part (if IZTRP is referenced) or the real part (if RZTRP is referenced) that equals FO. Returns the matching value from S as ANS.
BNTRP	Calculates polynomial coefficients needed for XNTRP interpolation.
NRRTS3	Finds real roots of a cubic equation.
SIZE (X,I,N), with entry point ORDER (X,I,N)	Loads the array I with indices from X array in the order of increasing X value. Rearranges X according to pointer array I.

Stream-Channel Data Preparation

RBIN	Reads in the stream-channel position and thickness arrays from a file with the identical format as the input of the TSONIC code (ref. 2).

BEST DOCUMENT AVAILABLE

FILLRB	Fills the arrays of radius and stream-tube thickness that correspond to the points in the solution grid by interpolating on the data from RBIN or by assuming a linear variation in the x direction.

Flow Solution

USONIC	Calculates the downstream boundary conditions, initializes the potential function, and relaxes the compressible potential flow equation on a given mesh until tolerance is reached. Calculates flow velocities on the blade surface when tolerance is reached.
FILPHI	Based on the coarse mesh solution for the potential, interpolates values for the next, finer mesh.

Output Generation

KEEPER (an entry point in USONIC)	Calculates and prints velocities, densities, pressures, and Mach numbers at all points in mesh. Records all results on file for later graphic display.

OPERATING INSTRUCTIONS

The information required to operate the mesh generators and flow solver consists first of a two-dimensional description of the blade shape in the stream surface. This is in the form of pairs of (x,y) points on the surface (fig. 6), together with parameters that describe the cascade layout (chord, stagger angle, and pitch). A group of parameters describing the desired density of the mesh lines completes the input for a geometry generation. To calculate the flow field, the upstream and downstream flow conditions, the rotational speed, the convergence criteria, and a schedule of meshes to be used should be input. If quasi-three-dimensional effects are to be included, a file containing a description of the stream channel's radial thickness and position as a function of distance along the stream surface is needed. The format for this file is identical to the input form for the code described in reference 2.

Output of QSONIC consists of printed listings, a formatted file with all generated mesh points, and a formatted file with final velocity components, Mach numbers, and pressures at all mesh points for use in graphic displays. The printed listing contains repeated input data, generated mesh coordinates on the blade, periodic progress reports on the flow convergence, and a list of the final velocities, pressures, and densities on the blade surface for each grid included in the schedule of solution meshes.

BEST DOCUMENT AVAILABLE

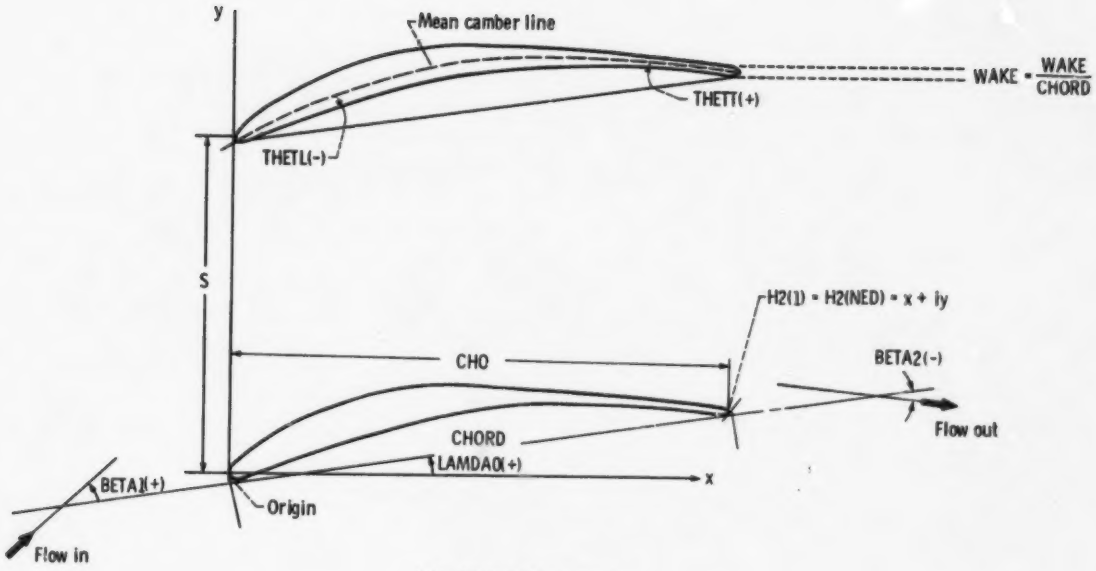

(a) In blade-to-blade surface.

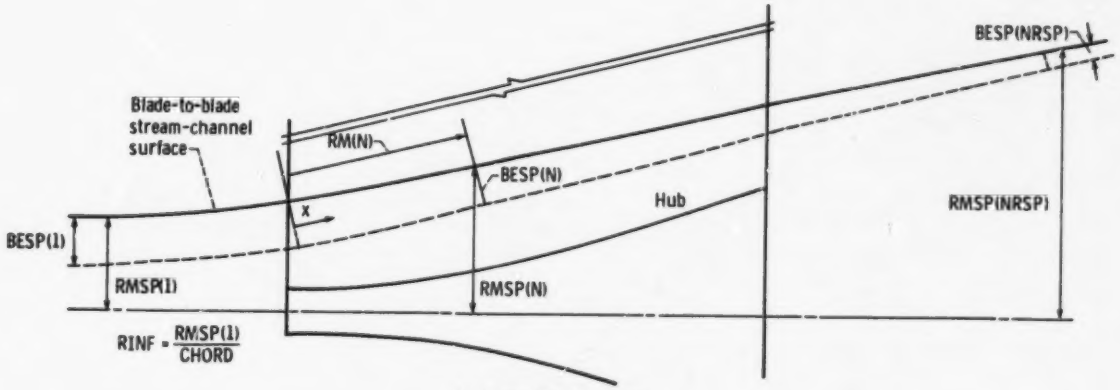

(b) In meridional surface.

Figure 6. - Geometric input variables.

BEST DOCUMENT AVAILABLE

Input/Output Files

I/O unit	Usage
2	File containing stream-channel data in TSONIC input format
5	Standard card input; NAMELISTS PARAMS, INSTUF
6	Standard printed output
8	Restart save file (read as unit 9 when restarting)
9	Restart input file, containing last successful print of potential values
13	For mesh generation runs, coordinates of all mesh points are written here for future solutions (4I5, followed by all 6E13.5). For flow solutions, x, y, velocities, pressures, and Mach numbers are recorded for later graphic display (4I5, 6E13.5).
18	Temporary storage
23	Previously developed mesh coordinates are read in from this file (= 13, from mesh generation runs).

Input

All input for any run will fall into the following categories:

(1) Logical and case control parameters (NAMELIST PARAMS, on unit 5)
(2) Bulk data input:
  (a) For geometry generation runs (NAMELIST INSTUF, on unit 5)
  (b) For flow solution runs:
    (i) Mesh point storage file (unit 23, equals output from geometry run)
   (ii) Stream-channel data file (unit 2)
  (iii) Restart input file (unit 9)

Logical and Case Control Parameters

Except for TITLE, the format for all of these variables is in NAMELIST form. The NAMELIST is PARAMS. If a default value is listed as none, a value of that parameter must be input. NAMELIST variables can be entered in random order.

Parameters applying to all runs. - The following parameters apply to all runs:

BEST DOCUMENT AVAILABLE

Name	Type	Default	Description
TITLE	Alphameric, (format, 20A4)	NONE	A one-line name for the case being run; TITLE must appear on the first line of unit 5.
NOFLOW	Logical	FALSE	=TRUE if run is to stop after generating a mesh (a geometry generation run).
RESTAR	Logical	FALSE	=TRUE if run is a continuation of a previous effort.
REMESH	Integer	4	Index in MS and NOZES arrays of the first grid to be used when restarting. Only flow solution runs may be restarted.
MS	Integer	NONE	Array (dimension 10) of values (maximum value, 25) for the number of grid lines that will enclose the blade. Twenty-five is a satisfactory number for blades of solidity near unity. As solidity increases, the maximum in MS should decrease to avoid crowding. Twenty-five allows five extra lines for high-camber blades (see CAMPER). The absolute limit is 30.
NOZES	Integer	NONE	Array (dimension 10) of values (maximum value, 49) for the number of grid lines radiating from the blade on one surface, starting with the line going to upstream infinity and ending with the line going to downstream infinity. Forty-nine radiating lines and 25 enclosing lines gave fairly square grid elements for solidities near 1. Maintaining similar aspect ratios between successive grids during a solution is a conservative rule to avoid convergence problems. If a value of NOZES is greater than zero, a mesh with that many lines will be developed and stored. If the value is negative, it is assumed that this mesh already exists on file and will be read in.
MESH1	Integer	1	Index in MS and NOZES of first grid to be calculated (geometry generation) and/or used for flow solution. MS and NOZES offer a choice of grids. For geometry generation runs, MESH1 selects one of these to be developed and stored, provided that NOZES (MESH1) > 0.

BEST DOCUMENT AVAILABLE

MESHN	Integer	NONE	Index in MS and NOZES of last grid to be calculated and/or used for flow solution. Normally, for geometry generation, MESHN = MESH1. Note: The purpose of a geometry generation run is to develop a grid of the maximum fineness desired. Subsequent flow solution runs can then solve the case on all grids listed in MS and NOZES between index MESH1 and MESHN by selecting an increasing number of the grid lines available on file ("grid refinement"). Grid refinement normally gives about a 30 percent gain in convergence speed over what can be attained by using the finest (stored) grid exclusively to meet a given convergence criterion. A schedule of three increasingly dense grids is usually sufficient. For flow solutions, MESH1 normally points to the coarsest mesh. To insure equal spacing of grid lines over the whole mesh, it is often helpful to require that $\frac{NOZES(I) - 1}{K^{(I-MESH1)}}$ be an integer, where MESH1 $\leq$ I $\leq$ MESHN, and K = 2, 3, 4, 5, etc. (i.e., K = 2 if number of grid lines is doubling between successive grids). A similar result holds for the values of MS. The logic of the code is much more general than these restrictions would indicate. However, whether the resulting grids would be suitable for flow solution is not certain.
LAMDAO	Real	NONE	Stagger or setting angle of the blade row, in degrees measured from the throughflow (x) direction to the blade chord line (clockwise negative). See figure 6.
CHORD	Real	NONE	True chord of the blade, in same units as blade coordinates.
S	Real	NONE	Blade spacing in y(rθ) direction, same units as coordinates.

Parameters required only for geometry generation. - There are two grid generators available, as decribed in reference 3. The electrostatic analog is applicable to any blade shape and to any value of stagger or turning. The interpolation scheme is good for most blades except knife edges (i.e.,

BEST DOCUMENT AVAILABLE

edge radius < 0.005 chord) or when the sum of stagger plus turning angles approaches 120°. Grid lines can be concentrated near the trailing edge or the periodic boundary or around the blade. No concentration is available when using the electrostatic analog. Refer to figure 6 for illustration of geometric input variables.

Parameters required for either grid generator:

Name	Type	Default	Description
NED	Integer	NONE	Total number of body definition coordinates to be input; one table of points with first point repeated as last point. See the section Bulk data for geometry runs. If NED < 0, no blade is read in and a flat-plate cascade is used.
KN	Integer	NONE	Flag to indicate which grid generator is to be used. For electrostatic analog, KN = 0 is input. For interpolation scheme, KN = number of body points on upper surface (from minimum to maximum x points, inclusive).

For the electrostatic analog generation, no other control parameters are needed. Refer to the section Bulk data for geometry runs for instructions on preparing the body points. Note: For this generator, the value from NOZES that is used must be odd.

Parameters applying only to interpolation scheme:

RLE	Real	NONE	Leading-edge radius of blade. Same units as coordinates. See figure 6.
RTE	Real	NONE	Trailing-edge radius of blade. Same units as coordinates.
THETL	Real	0	Camber angle of leading edge, deg, measured from the aerodynamic chord to the line tangent to the mean camber curve at the leading edge. Clockwise is positive.
THETT	Real	0	Camber angle at trailing edge, deg, measured from chord line to the line tangent to mean camber curve at the trailing edge. Clockwise is positive. Specification of THETT and THETL gives better interpolation results for thin blades with high camber.

BEST DOCUMENT AVAILABLE

CAMPER	Integer	6	For blades whose chordline lies outside the blade, extra grid lines surrounding the blade are needed to interpolate the blade position. The truncated value of MS( )/CAMPER is added to MS( ). The maximum allowed value of MS( ) + MS( )/ CAMPER is 30 grid lines (see MS).
STABAC	Real	0.999	For test cases where no blade shape is to be input (NED < 0) and if STABAC = 0.999, a flat-plate grid is developed. For 0. < STABAC < 0.999, one of the surrounding grid lines will be designated as a body shape and a mesh developed around it. As STABAC approaches zero, the grid line designated is ever closer to the periodic boundary.
CHOP	Real	0.99	Fraction of distance from midchord to either end beyond which all lines that intersect the flat plate near the leading or trailing edge will receive special handling to calculate the point where they intersect the blade shape. This is often necessary for blades with small leading- or trailing-edge radii (less than 2 percent chord). Normally, 0.9 < CHOP < 1.0.
SMOOTH	Logical	False	= TRUE. for automatic addition of more blade definition points in the region of both leading and trailing edges. Recommended for all blades except cusps and wedges.
LEONLY	Logical	False	= TRUE. for smoothing about leading edge only, for the case where only the trailing edge has a cusp or wedge. Smooth must also be .TRUE.
SLP1	Real	1.	If SLP1 < 0., concentration of grid lines is desired in some region of the mesh. These four parameters control the amount and location of the concentration. If SLP1 < 0., its absolute value and that of SLP2 refer to the end-point slopes on a fifth-power polynomial curve of the new values of ζ (referred to as ζ' in fig. 7) as a function of the original values of ζ, where ζ-lines are those that radiate from the blade; but if SLP2 is also less than 0., its absolute value is interpreted as $d\zeta'/d\zeta\|_{FK}$, where FK' is the value of ζ at the trailing edge. A small
SLP2	Real	2.	
SLP3	Real	1.	
SLP4	Real	1.	

BEST DOCUMENT AVAILABLE

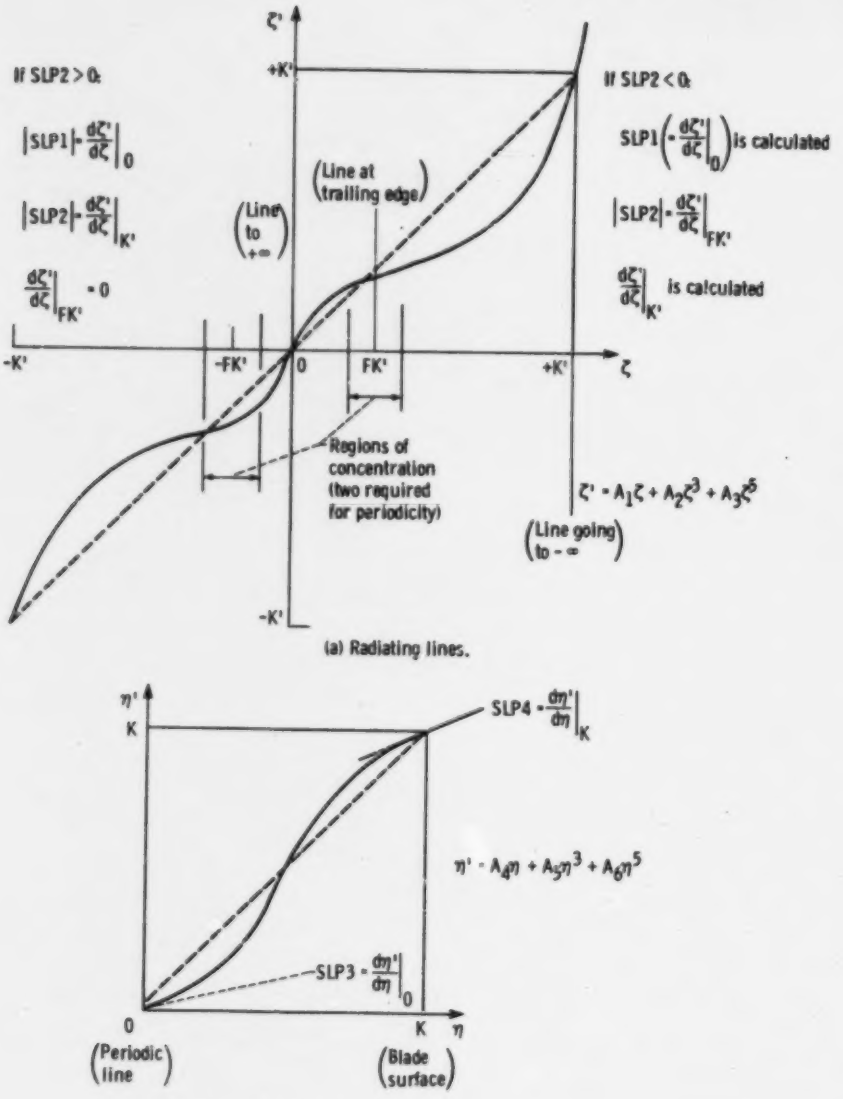

(a) Radiating lines.

(b) Surrounding contours.

Figure 7. - Polynomial curves used for concentration of grid lines.

value of |SLP2| in this case results in a flatter curve in the trailing-edge region, thus concentrating more values of ζ' in that region. If the concentration is not desired at the trailing edge, the value of F (the variable name for F is EF), between 0. and 1., which determines the point of concentration on the blade, can be adjusted by manipulating input values of SLP1 and SLP2 as shown in the following table. Exact control is not available in this version of the code. Hence concentration should be used cautiously.

BEST DOCUMENT AVAILABLE

Near line going to	Value of EF	Input SLP1	Input SLP2
$+\infty$	0	--------	-------
	.25	-1.533	+17.
	.5	-1.667	+5.
	.75	-2.1428	+2.777
$-\infty$	.99	-26.	+2.02

SLP3 and SLP4 refer to the end-point slopes on a similar curve of new values for η (η' in fig. 7) as a function of the old η values. SLP3 and SLP4 would normally be less than 1., since concentration near the end points (periodic line and body) is desired for η.

Parameters required only for flow solution runs. - The following parameters are required only for flow solution runs:

Name	Type	Default	Description
MINF	Real	NONE	Mach number at upstream boundary. For rotors this is the relative Mach number. If the downstream Mach number is known to be supersonic, input MINF with a minus sign.
BETA1	Real	NONE	Flow angle at upstream boundary, deg. For rotors this is the angle in the relative frame. BETA1 is measured from the aerodynamic chordline to the direction of flow. Clockwise is negative.
BETA2	Real	NONE	Flow angle at downstream boundary, deg, measured from aerodynamic chordline to direction of flow. Clockwise is negative. For rotors this is the angle in the relative frame.
GAMMA	Real	1.4	Ratio of specific heats
TOLS	Real	NONE	Array (dimension 10) of tolerances corresponding to MS and NOZES. Each grid solution will proceed until its TOLS value is satisfied. There are three forms of input permitted:

BEST DOCUMENT AVAILABLE

(1) -1. < TOLS(I) < 0.: Proceed until the relative circulation error $|(C_{calc} - C_{exact})/C_{exact}|$ is less than $|TOLS(I)|$. This is appropriate only for lifting (nonsymmetric) cases and is indicative only of convergence in the trailing-edge region. TOLS values between -10^{-3} and -10^{-6} are typical for most grids with the input value approaching zero as the mesh becomes finer.

(2) 0. < TOLS(I) < 1.: Proceed until the average relative change in potential on the mesh $(\delta\varphi/\varphi)_{av}$ is less than $|TOLS(I)|$. This is a more rigorous criterion but slower to be met because of the averaging of all grid points. Values typically should be between 10^{-3} and 10^{-5}. There is no benefit to lingering on the coarser grids much after the average correction has leveled off.

(3) 1. < TOLS(I): Proceed until the number of iterations equals TOLS(I). Regardless of the TOLS input, each grid solution will terminate after 300 iterations if the TOLS criterion has not yet been met.

OVEREL	Real	1.5	Overrelaxation parameter, 1. < ω < 2., for all subsonic points in the mesh
UNDERL	Real	1.	Underrelaxation parameter between 0.5 and OVEREL. During the first few iterations on each grid ω is changed gradually from UNDERL to OVEREL. Default is usually adequate.
SUPREL	Real	1.	Overrelaxation parameter applied to supersonic points. Maximum value, 2.0.
NOWREL	Integer	20	Number of iterations on each grid before subsonic overrelaxation is applied. Normally 2 < NOWREL $\leq$ 20.
NOTYET	Integer	2	Number of iterations on each grid before compressibility effects ($\rho/\rho_{in} \neq 1.$) are allowed. SUPREL is also turned on after this many iterations. Normally 2 < NOTYET $\leq$ 10. If NOWREL > NOTYET, UNDERL is not used.

BEST DOCUMENT AVAILABLE

TEGARD	Real	2.0	Default is adequate, except for high-speed blades with a wedge or small radius in the leading- or trailing-edge region. Increases damping in edge regions. Use cautiously in combination with DAMP to avoid instability. $1. \leq$ TEGARD $< 10.$
DAMP	Real	1.0	Multiplier on artificial density correction term, to increase damping. Maximum, 2.0. Intended to reduce overshoot on midblade shocks.
CII	Real	0.2	To improve stability for multiple-grid cases, SUPREL is reduced by an amount equal to CII for each successive grid until SUPREL = 0.5.
IT	Integer	10	Number of iterations between intermediate printouts of residuals and Mach number and between updates of the densities used in equation (21).
ALLOUT	Logical	FALSE	=TRUE. to list flow quantities at all grid points on the last mesh.
QUASI3	Logical	FALSE	=.TRUE. to activate stream-channel thickness and/or radius variations.
NSTRM	Integer	1	Logical position of desired stream-surface data on the stream-channel file. See the section Bulk data for flow solution runs.
RINF	Real	1.	Spanwise radius at upstream boundary divided by aerodynamic chord. Radius effects are activated if RINF $\neq$ 1. With the current version of the code, the following cases are allowed:

QUASI3	RINF	Results
.F.	1.	Planar two-dimensional
.T.	≠1.	Thickness on file Radius on file
.T.	1.	Thickness on file Constant radius

WAKE	Real	0.	Thickness of a wake, as a fraction of aerodynamic chord. Used only in calculation of downstream Mach number to simulate a blockage.

BEST DOCUMENT AVAILABLE

MINF2	Real	10.0	Downstream Mach number. If any value is input other than 10., it is used as M_{out}. Otherwise, M_{out} is calculated by using equation (27). MINF2 is available as another means of introducing blockage (see WAKE) or to compare a run with other analyses. Also, because of the behavior of the function F in equation (27) near sonic speeds, it is often necessary to input the downstream Mach number here and to avoid use of equation (27) if M_{out} is known to be near 1.0.
OMEGA	Real	0.	For rotors, wheel rotation is in radians per second. If blade row is moving down along y axis, OMEGA < 0.
VAXIAL	Real	999.	Must be input if OMEGA ≠ 0. VAXIAL is the upstream velocity component in the streamwise (x) direction divided by the aerodynamic chord. VAXIAL = $V_{x_{in}}$ /C. Units are $(\text{seconds})^{-1}$.
FLOCO	Real	999.	For rotors, wheel speed can be input by using OMEGA and VAXIAL or as FLOCO, the flow coefficient at the upstream boundary. FLOCO = $V_{x_{in}}$ /U, where U is wheel speed. If OMEGA is used for input, FLOCO should be left as 999. It will be calculated as $$\text{FLOCO} = \frac{\text{VAXIAL}}{\text{OMEGA} \cdot \text{RINF}}$$

Bulk Data Input

Bulk data for geometry runs. - The format for all variables listed here is namelist form. The namelist is INSTUF.

Name	Type	Default	Description
H2	Complex	NONE	Table of all blade definition points. The real part is the x coordinate and the imaginary part is the y coordinate. The table should begin at the point of maximum x value (near the trailing edge) and proceed clockwise back around to the first point, which is repeated. The blade must be at stagger angle and the origin near the point of minimum x. For electrostatic analog grids the stagger angle must be positive (i.e.,

BEST DOCUMENT AVAILABLE

			the leading edge is low, and the trailing edge is high). The maximum number of points in H2 is 99 for the interpolation scheme or 63 for the electrostatic analog.
BUG2	Logical	FALSE	= .TRUE. for a more detailed output list of the geometry generation run, including second derivatives at grid points on the body.

Bulk data for flow solution runs. - The mesh point storage file (unit 23) is a required input only if a mesh is not generated in the same run as the flow solution. The stream-channel data file (unit 2) is required only if quasi-three-dimensional effects are to be calculated.

Mesh point storage file: If the mesh point file is needed, the values of NOZES to be used must be negative. The file is written by a geometry generation run as unit 13. The first record is 2I5, with the first position being the value of NOZES for which the grid was generated and the second position being the value of MS used. All other records are formatted 6E13.5 and contain the x values at all points in the mesh, followed by all y values. The sequence for both is to begin on the periodic boundary at the line going to upstream infinity (nominal) and then to proceed clockwise around each ellipse-like curve, repeating the first point, moving in to the next ellipse, and continuing until the blade surface has been listed in the same way. The orientation of the x,y points is with the aerodynamic chord along the x axis and the origin at midchord. The statements that create this file in subroutine WRAPUP have the form:

```
      WRITE (13,1) NOZ, M, KN, NED
      WRITE (13,2) ((X(I,J), I = 1, NZZ), J = 1,M), ((Y(I,J),I = 1, NZZ),
        J = 1,M), (ETA(I), I = 1, NZZ), (ZETA(J), J = 1,M)
    1 FORMAT (4I5)
    2 FORMAT (6E13.5)
```

Stream-channel data file: If the stream-channel data file is required, QUASI3 must be .TRUE. The file must contain a table of stream-tube thicknesses, radial positions, and corresponding x values along the stream surface. The format is identical to that shown on page 18 of reference 2. However, not all of these data are necessary for QSONIC. The following list and figure 8 show the minimum requirements for the data needed by QSONIC. If more than one such set of data exists on the file, NSTRM is used to select the desired set. (See the section TEST CASE.)

Record number	Column number	Name	Type	Default	Description
1	BLANK				
2	BLANK				
3	21-30	CHO	REAL	NONE	Aerodynamic chord multiplied by the cosine of LAMDAO
4	BLANK				

BEST DOCUMENT AVAILABLE

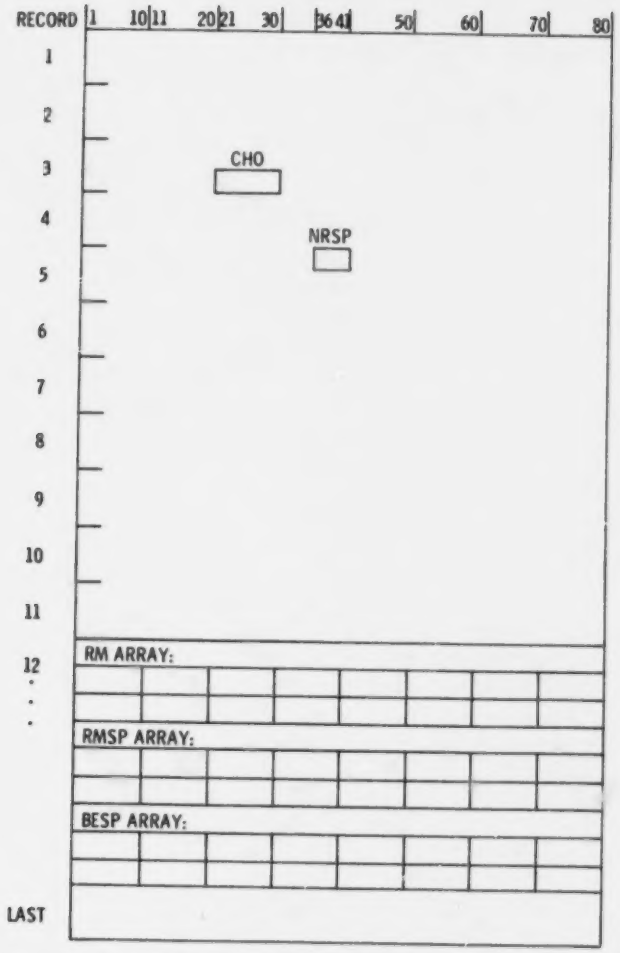

Figure 8. - Minimum stream-channel data required, in TSONIC format.

5	36-40	NRSP	INTEGER	NONE	Total number of data points in each of the tables of thickness, radial position, and x locations. If NRSP = 2, a linear distribution is obtained between the end points given.
6 7 8 9 10 11	BLANK				
12 to conclusion	1-80 (8F10.5)	RM	REAL	NONE	Array of corresponding x locations for thickness and radius data values. For a blade sitting at the proper stagger angle,

BEST DOCUMENT AVAILABLE

					x = 0 at the blade leading edge. Units can be any consistent length scale common to CHO, RM, RMSP, and BESP.
	1-80 (8F10.5)	RMSP	REAL	NONE	Spanwise radial positions of stream surface at given x locations.
	1-80 (8F10.5)	BESP	REAL	NONE	Array of stream-tube thickness values at the given x locations.
LAST	BLANK				

Restart input file: This is required if RESTAR = .TRUE. This file was written by the code during the interrupted run. It contains the field of potential values in 6E13.5 format and is updated whenever a new grid is begun (if more than one was requested with MESH1 ≠ MESHN) and also at intervals of the iteration count divisible by the input parameter IT.

Caution: Restart capabilities have not been fully tested in version 1.5 of the code.

Output

All output produced by this program falls into the following categories:

(1) Geometry generation run output
  (a) Printed listing (unit 6)
  (b) Mesh points file (unit 13)
(2) Flow solution run output
  (a) Printed listing (unit 6)
  (b) Restart save file (unit 8)
  (c) Plot data save file (unit 13)

Refer to the test case in the next section for examples of the printed list outputs.

Geometry Generation Run Outputs

Printed listing. - The output list on unit 6 will contain the following items:

(1) Title of case, as entered on input

(2) The phrase CASE CONTROL INPUT ECHO, followed by a namelist output of the input data as entered with NAMELIST PARAMS. All variable names are identical to those described in the INPUT section.

(3) For the interpolation scheme the phrase INTERPOLATION SCHEME GRID GENERATED, followed by any conditional messages as described in the section on error messages

(4) For the electrostatic analog the phrase ELECTROSTATIC ANALOG GRID GENERATED, followed by
  (a) The phrase NEGRID = , followed by the value of MS used for this grid
  (b) The phrase NZGRID, ODD = , followed by the value of NOZES used for this grid.

BEST DOCUMENT AVAILABLE

(c) The phrase IMAXY = , followed by the index of the point with the maximum y value
(d) The phrase SURFACE COORDINATES, followed by a two-column list (x, then y) of the blade coordinates as obtained from NAMELIST INSTUF
(e) The phrase NUMBER OF BODY POINTS = , followed by the total number input from INSTUF
(f) The phrase PITCH = , followed by input value of S divided by CHORD
(g) The phrase CHO = , followed by the value of CHORD * COS(LAMDAO)
(h) The phrase STAGGER = , followed by the value of LAMDAO in degrees
(i) The phrase ITER COUNT FOR INTERNAL GRID POINTS = , followed by the number of iterations required to obtain all points between the periodic boundary and the blade
(j) The phrase ERR = , followed by the average residual for this iteration

(5) If BUG2 = .TRUE., these additional outputs and phrases will be listed for either grid generator:
(a) NOZ = , followed by the value of NOZES used
(b) M = , followed by the value of MS used
(c) KN = , followed by number of blade definition points on upper surface of blade after going through the smoothing routine (smoothing done only for Interpolation scheme grids)
(d) NED = , followed by the total blade definition points after smoothing
(e) A list of smoothed blade definition points along with calculated second derivatives. For electrostatic analog grids, blade orientation is the same as described under parameter H2 in the input section. For interpolation scheme grids, it is the same as described in item (5h).
(f) All x grid points are listed as they appear on the mesh points storage file
(g) All y grid points are then listed in a similar manner
(h) Final calculated grid points that lie on the blade are listed along with calculated second derivatives. The orientation of the blade (interpolation scheme) is with the chord horizontal and the origin at midchord. For electrostatic analog grids, orientation is the same as on input.

(6) Final calculated grid points that lie on the blade are listed. Orientation is with the chord at stagger and the origin at midchord.

Mesh points file. - The mesh points file is written on unit 13 and contains one record (2I5) with the values of NOZES and MS used in generating the grid, followed by all x values, then all y values, in 6E13.5 format. No user intervention is required to use the file as bulk input for a future flow solution run (unit 23). It is also useful as plot input for preliminary grid views.

Flow Solution Run Output

Printed listing. - The printed listing is similar to grid generation runs for the first two items:

BEST DOCUMENT AVAILABLE

(1) Title of case
(2) The phrase CASE CONTROL INPUT ECHO, followed by namelist list
(3) For cases with rotation (OMEGA > 0. or FLOCO ≠ 999.) the phrase ROTATION EFFECTS INCLUDED, ABSOLUTE AND RELATIVE TRIANGLES HAVE -, followed by a NAMELIST output of the following velocity triangle parameters:

MINF	Input value of relative Mach number (relative to the frame fixed to blade)
MINF2	Relative Mach number downstream as calculated or input
QINF2	Relative speed downstream, $q\ rel_{out}/q\ rel_{in}$ with $q\ rel_{in} = 1$; where $q = (u^2 + v^2)^{1/2}$
ABETA1	Absolute inlet flow angle measured from throughflow (x) direction to actual flow direction, where clockwise is negative
ABETA2	Absolute outlet flow angle at downstream boundary
AQINF1	Upstream speed ratio, absolute to relative, $q\ abs_{in}/q\ rel_{in}$
AQINF2	Downstream speed ratio, $q\ abs_{out}/q\ rel_{in}$
AMINF	Absolute upstream Mach number (subtracting wheel speed from MINF)
AEM	Absolute downstream Mach number
ROTATN	Wheel speed as calculated from FLOCO and BETA1 normalized by assuming $q\ rel_{in} = 1$. ROTATN = cos (BETA1 + LAMDAO)/FLOCO.

For all flow cases:

(4) The phrase CALCULATED FLOW PARAMETERS, followed by a Namelist output of these calculated downstream conditions:

CIRCLN	Exact circulation for given inlet and outlet flow angles
MINF2	Relative Mach number downstream as calculated or input
B2OB1	Ratio of downstream channel thickness to upstream thickness, as input or as obtained from stream-channel data file
R2OR1	Ratio of downstream spanwise radial position of stream-channel to upstream position, as input or as obtained from stream-channel data file
RINF	Spanwise radius at upstream boundary divided by aerodynamic chord, as input

BEST DOCUMENT AVAILABLE

RATLE — Calculated radius at leading edge of blade based on radius distribution from stream-channel data file or the linear distribution

For each grid selected for relaxation,

(5) A table of intermediate results is printed at intervals whenever the iteration count is divisible by IT. The table consists of the following:

AVERAGE PHI CORRECTN	$\sum_{1}^{N} \delta\varphi \Big/ N_{\varphi typical}$
RESIDUAL AT T•E•	Net mass flow out of finite volume element at trailing edge
MAX MACH ON BLADE	M_{max} on blade surface, not including points in the first and last 6 percent of blade chord
CALCULATED CIRCULATION	$C_c = (\varphi_{last} - \varphi_{1})_{on\ blade}$ line
RELATIVE CIRC ERROR	$(C_c - C_{exact})/C_{exact}$, where C_{exact} = CIRCLN
SUBSONIC RELAX FAC.	OVEREL, as input, subject to delay by NOWREL
SUPERSONIC RELAX FAC.	SUPREL, as input, subject to reduction by CII and delay by NOTYET

(6) For each grid selected for relaxation, a table of final flow calculation on blade surface, including X/CX, Y/CX, X, Y, MACH, STATIC PRES COEF, PHI, XVEL, YVEL, and DENSITY, where CX = CHORD * (COS LAMDAO), PHI denotes the potential field values, XVEL and YVEL are velocity components normalized to $u_{in}^2 + v_{in}^2 = 1$, and density is normalized to $\rho_{in} = 1$.

(7) For each grid selected for relaxation, after all grids have been solved, and if ALLOUT = .TRUE., a table of flow variables at all grid points is printed, beginning with the phrase CALCULATED FLOW FIELD AT ALL GRID POINTS. All variables are the same as in the previous table (item 6) with the addition of FLOW ANGLE = $\tan^{-1}$ YVEL/XVEL in degrees.

Restart save file. - See section Bulk data for flow solutions runs for a description of this file, written on unit 8.

Plot data save file. - At the completion of the table of the flow field at all grid points, or immediately after the last grid is complete if ALLOUT = .FALSE., the following information is recorded on unit 13:

BEST DOCUMENT AVAILABLE

Record number	Format	Data
1	215	NOZ,M values of NOZES and MS on final grid used. Total number of grid points = (2 * NOZ - 1) * (M) = NOO * M = NTOT
2 → $\frac{NTOT}{6}$	6E13.5	((X(I,J),I = 1,NOO),J = 1,M), throughflow coordinates. Blade is at stagger. Origin is at midchord.
→ 2 $\frac{NTOT}{6}$		((Y(I,J),I = 1,NOO),J = 1,M), tangential coordinates
→ 3 $\frac{NTOT}{6}$		((XVEL(I,J),I = NOO),J = 1,M), throughflow velocity components
→ 4 $\frac{NTOT}{6}$		((YVEL(I,J),I = NOO),J = 1,M), tangential velocity components
→ 5 $\frac{NTOT}{6}$		((MACH(I,J),I = NOO),J = 1,M), Mach numbers
→ 6 $\frac{NTOT}{6}$		((PRES(I,J),I = NOO),J = 1,M), static pressure coefficients

If a flow solution and geometry generation are combined in one run, this plot data will overwrite the mesh points (also unit 13) written by the grid generator. The graphic output shown with the sample test case was generated by a local graphics package at NASA Lewis that accessed a PLOT data file such as this.

Error and Condition Messages

Module	Message phrase	Description
XYCALC	SGEN FAILED. IBAD=	In attempting to smooth a table of input data, the module that calculates the value of the distance along the curves detected a large change in slope between adjacent point pairs at the table index number of IBAD. Remedy: If the output grid points are unsatisfactory, check the data going into XYCALC for any points out of sequence, repeated points, all-zero data, etc.
XYCALC	SPGEN UNABLE TO COMPLETE SEGMENT	The module that calculates new points on the curve to smooth the data could not satisfy the point spacing criteria listed in the SPGEN subroutine. Remedy: Improve the input data (i.e., add more points if necessary) so as to avoid any large changes in slope (>90°) between adjacent points. Also, check the data for discrepancies as noted for the previous message.

BEST DOCUMENT AVAILABLE

The following four messages refer to line numbers 'I'. While a mesh is being generated, radiating lines are numbered beginning with the line to upstream infinity and proceeding clockwise around the blade.

SURFUP	ITERATION PROCEEDS WITH SMOOTHER SLOPE DATA FOR LINE 'I'	After 20 attempts to find the intersection of the blade surface and radiating line 'I', the table of x and y values versus n (surrounding contours) on line 'I' is smoothed by using subroutine XYCALC, and the iteration is attempted again.
SURFUP	ITERATION FAILED FOR LINE 'I'. PROCEEDING TO EDGE REGION TECHNIQUE	When the total iteration attempts mentioned above reach 50 or they become divergent, the solution of this line is put aside until all others are completed. At that time the intersection point is found by interpolating on the table of intersection points formed by all the successful iterations. This is referred to in the code as the "edge region technique," because this is normally required in the leading- and trailing-edge regions of sharp blades.
SURFUP	ITERATION NOT ATTEMPTED FOR LINE 'I'. BODY X TOO CLOSE TO LE OR TE: 'XB XP' PROCEED TO EDGE TECH."	(See explanation of CHOP parameter in the section on geometry parameters.) If X = XB (where XB is the intersection of radiating line 'I' with the X axis) is larger in absolute value than the quantity CHOP*XP (where XP is equal to the half-chord length of the flat plate), this line is assumed to be near a sharp tip region on the blade and the normal iteration procedure is bypassed. This message should be expected if CHOP < 0.95.
SURFUP	GRID LINE NO. 'I' HAS DEGENERATED TO POINT. TRY THETL,THETT = LE,TE CAMBER ANGLES.	For certain high-camber blades with small tip radii, the stretching of the grid to include the blade can degenerate if the camber information is not available at the leading and trailing edges. See THETL and THETT parameter definitions in the section on geometry inputs.

All other messages are self-explanatory or not critical to code success.

TEST CASE

The execution times for the following sample case, run on an IBM 3033, were

(1) Interpolation scheme grid generation, 40 seconds for 2500 grid points or
(2) Electrostatic grid generation, 30 seconds and
(3) Quasi-three-dimensional flow solution on three consecutively finer meshes, 260 seconds

BEST DOCUMENT AVAILABLE

The blade geometry is the hub section of the Sanz supercritical compressor stator designed for NASA Lewis by using the methods of reference 6. A good comparison between QSONIC and the original hodograph design solution is presented in reference 3 for a planar two-dimensional flow.

Input - Case Control Parameters for Interpolation Scheme Grid Generation

```
        SANZ SUPERCRITICAL STATOR HUB SECTION, GRID GENERATION RUN
&PARAMS S=.863,MSTRM=3,RINF=1.724,
MESH1=4,MESHM=4,GLASI3=.FALSE.,
 MS=3,7,13,25,MOZES=-9,-13.-25,49,
 NOFLOW=.TRUE.,
TOLS=1.E04,-2.E-05,
 7.E-05,4.E-05,-.000001,2*0.,
 BETA1=29.1,NOWREL=20,NOTYET=10,
 BETA2=-19.6,LSMDA0=19.5,
 OVEREL=1.4,CII=.4,MINF=.801,
 IT=30,ALLOUT=.TRUE.,SUPREL=2.0,SMOOTH=.TRUE.
BLE=.007,BTE=.029,KN=62,NED=68,CHORD=1.0144
&END
```

Bulk Data Input for Geometry Generation

```
&INSTUF
M1= 100*(0.0, 0.0),
M2= (0.94980, 0.35220999), (0.9482999, 0.342498), (0.9342999, 0.329498),
    (.9182999,0.321498),
(0.9072999, 0.32149999), (0.8672999, 0.321998), (0.8034999, 0.323198),
    (.6818999,0.3144),
(0.5879999, 0.295998), (0.5217999, 0.27638), (0.4682999, 0.2548),
    (.4284999,.238498),
(0.3942999, 0.22168), (0.3675999, 0.20729999), (0.3458999, 0.19128),
    (.2519999,.136898),
(0.2052999, 0.10628), (0.1971999, 0.74999988E-01), (0.1088999, 0.4388E-01),
(0.82199993E-01, 0.2868E-01), (0.6148E-01, 0.1688E-01),
    (0.03989999,0.0063999997),
(0.2889999E-01, 0.1199999E-02), (0.17899998E-01, -0.258E-02),
    (.01259999,-.0036),
(0.72999978E-02, -0.368E-02), (0.0, 0.0), (-0.10000178E-01, 0.71999958E-02),
(0.39999978E-02, 0.20138E-01), (0.168E-01, 0.4988E-01),
    (.03529999,.064699995),
(0.6869996E-01, 0.10059999), (0.1138999, 0.143898), (0.1397999, 0.18198),
(0.1867599, 0.2074198), (0.20848, 0.22428), (0.225398, 0.2367898),
    (.2392299,.2465798),
(0.2507299, 0.25438998), (0.2607099, 0.260958), (0.26959, 0.26654999),
    (.2773799,.2714398),
(0.2844899, 0.27571998), (0.2904699, 0.2795398), (0.2969099, 0.2829498),
    (.3023999,.2860298),
(0.3074799, 0.2888198), (0.3122399, 0.2913798), (0.316688, 0.293718),
    (.3208599,.2958699),
(0.3247699, 0.2978598), (0.3283899, 0.2997298), (0.3320799, 0.3014698),
    (.335518,.30319998),
(0.33888, 0.3046698), (0.3419899, 0.30613998), (0.3496699, 0.3079598),
    (.3488799,.308998),
(0.3518199, 0.310278), (0.3539199, 0.3114698), (0.356758, 0.3126698),
    (.3595399,.3138498),
(0.3622699, 0.31495998), (0.364968, 0.3160598), (0.3675599, 0.3170998),
    (.3701199,.3180998),
(0.37248, 0.31901998), (0.375018, 0.3199598), (0.3773299, 0.3206618),
    (.3795499,.3216298),
(0.3816999, 0.3223998), (0.3838699, 0.3231498), (0.3861299, 0.3239298),
    (.4081899,.3285498),
(0.40748, 0.330668), (0.4084999, 0.343398), (0.5118999, 0.392798),
    (.5442999,.360298),
(0.6174999, 0.365398), (0.6926999, 0.372298), (0.7486999, 0.378998),
    (.8201999,.3795),
(0.8772999, 0.381498), (0.9072999, 0.382398), (0.9172999, 0.38258),
    (.93338,.3796),
(0.94738, 0.364498), (0.94980, 0.35220999), 12*(0.0, 0.0),
BUGZ= F,
&END
```

BEST DOCUMENT AVAILABLE

Printed Output List for Geometry Generation

```
 QSONIC VERSION 1.5                    SANZ SUPERCRITICAL STATOR HUB SECTION,  GEOMETRY GEN

     CASE CONTROL INPUT ECHO

 &PARAMS
 NOFLOW= T
 RESTAR= F
 REMESH= 4
 MS= 3, 7, 13, 25, 6*0
 NOZES= -9, -13, -25, 49, 6*0
 MESH1= 4
 MESHN= 4
 LAMDA0= 19.50
 CHORD= 1.01460
 S= 0.8630
 NED= 88
 KN= 62
 RLE= 0.6999999E-02
 RTE= 0.290E-01
 THETL= 0.0
 THETT= 0.0
 CAMPER= 6
 STABAC= 0.9990
 CHOP= 0.9899999
 SMOOTH= T
 LEONLY= F
 SLP1= 1.0
 SLP2= 2.0
 SLP3= 1.0
 SLP4= 1.0
 MINF= 0.8010
 BETA1= 25.09999
 BETA2= -15.60
 GAMMA= 1.40
 TOLS= 10000.0, -0.1999999E-04, 0.6999999E-04, 0.5999999E-04, -0.9999994E-06
 5*0.0
 OVEREL= 1.599999
 UNDERL= 1.0
 SUPREL= 2.0
 NOWREL= 20
 NOTYET= 10
 TEGAMD= 2.0
 DAMP= 1.0
 CII= 0.40
 IT= 30
 ALLOUT= T
 QUASI3= F
 NSTPM= 3
 RINF= 3.7240
 WAKE= 0.0
 OMEGA= 0.0
 VAXIAL= 0.0
 FLOCO= 999.0
 MINF2= 10.0
 BIGLAX= F
 &END


                                        INTERPOLATION SCHEME GRID GENERATED
 SGEN FAILED.  IBAD=  30
 ITERATION PROCEEDS WITH SMOOTHER SLOPE DATA FOR LINE   43
 ITERATION PROCEEDS WITH SMOOTHER SLOPE DATA FOR LINE   44
 ITERATION FAILD FOR LINE   44 PROCEEDING TO EDGE REGION TECHNIQUE
 ITERATION NOT ATTEMPTED FOR LINE   45, BODY X TOO CLOSE TO LE OR TE:    0.488165E 00   0.491130E 00 PROCEED TO EDGE TECH.
 ITERATION NOT ATTEMPTED FOR LINE   46, BODY X TOO CLOSE TO LE OR TE:    0.489080E 00   0.491130E 00 PROCEED TO EDGE TECH.
 ITERATION NOT ATTEMPTED FOR LINE   47, BODY X TOO CLOSE TO LE OR TE:    0.487084E 00   0.491130E 00 PROCEED TO EDGE TECH.
 ITERATION NOT ATTEMPTED FOR LINE   93, BODY X TOO CLOSE TO LE OR TE:   -0.488160E 00   0.491130E 00 PROCEED TO EDGE TECH.
 ITERATION NOT ATTEMPTED FOR LINE   94, BODY X TOO CLOSE TO LE OR TE:   -0.489081E 00   0.491130E 00 PROCEED TO EDGE TECH.
 ITERATION NOT ATTEMPTED FOR LINE   95, BODY X TOO CLOSE TO LE OR TE:   -0.487099E 00   0.491130E 00 PROCEED TO EDGE TECH.
 SGEN FAILED.  IBAD=  21
```

BEST DOCUMENT AVAILABLE

GRID OUTPUT POINTS ON BLADE SURFACE, CHORD AT STAGGER ANGLE

I	X	Y
0	0.45668E 00	0.15691E 00
1	0.44927E 00	0.15345E 00
2	0.43797E 00	0.15170E 00
3	0.42350E 00	0.15180E 00
4	0.40665E 00	0.15197E 00
5	0.38739E 00	0.15221E 00
6	0.36596E 00	0.15272E 00
7	0.34264E 00	0.15328E 00
8	0.31783E 00	0.15326E 00
9	0.29187E 00	0.15244E 00
10	0.26499E 00	0.15094E 00
11	0.23748E 00	0.14860E 00
12	0.20961E 00	0.14530E 00
13	0.18160E 00	0.14100E 00
14	0.15360E 00	0.13576E 00
15	0.12576E 00	0.12961E 00
16	0.98172E-01	0.12256E 00
17	0.70919E-01	0.11464E 00
18	0.44072E-01	0.10585E 00
19	0.17699E-01	0.96168E-01
20	-0.82057E-02	0.85733E-01
21	-0.33653E-01	0.74616E-01
22	-0.58602E-01	0.62837E-01
23	-0.83080E-01	0.50458E-01
24	-0.10701E 00	0.37493E-01
25	-0.13050E 00	0.24146E-01
26	-0.15353E 00	0.10458E-01
27	-0.17608E 00	-0.34693E-02
28	-0.19820E 00	-0.17469E-01
29	-0.21983E 00	-0.31533E-01
30	-0.24109E 00	-0.45432E-01
31	-0.26181E 00	-0.59060E-01
32	-0.28200E 00	-0.72396E-01
33	-0.30164E 00	-0.85332E-01
34	-0.32071E 00	-0.97631E-01
35	-0.33911E 00	-0.10929E 00
36	-0.35678E 00	-0.12017E 00
37	-0.37360E 00	-0.13018E 00
38	-0.38943E 00	-0.13943E 00
39	-0.40411E 00	-0.14766E 00
40	-0.41773E 00	-0.15448E 00
41	-0.42976E 00	-0.16019E 00
42	-0.44028E 00	-0.16492E 00
43	-0.44929E 00	-0.16776E 00
44	-0.45658E 00	-0.16885E 00
45	-0.46225E 00	-0.16779E 00
46	-0.46645E 00	-0.16457E 00
47	-0.46838E 00	-0.15846E 00
48	-0.46450E 00	-0.15070E 00
49	-0.46045E 00	-0.14111E 00
50	-0.45376E 00	-0.12980E 00
51	-0.44455E 00	-0.11689E 00
52	-0.43276E 00	-0.10285E 00
53	-0.41890E 00	-0.87286E-01
54	-0.40309E 00	-0.70493E-01
55	-0.38557E 00	-0.52916E-01
56	-0.36655E 00	-0.34465E-01
57	-0.34618E 00	-0.15481E-01
58	-0.32471E 00	0.37890E-02
59	-0.30223E 00	0.22980E-01
60	-0.27893E 00	0.41877E-01
61	-0.25496E 00	0.60262E-01
62	-0.23043E 00	0.77926E-01
63	-0.20541E 00	0.94578E-01
64	-0.17998E 00	0.11009E 00
65	-0.15421E 00	0.12432E 00
66	-0.12812E 00	0.13713E 00
67	-0.10166E 00	0.14815E 00
68	-0.74903E-01	0.15748E 00
69	-0.47949E-01	0.16538E 00
70	-0.20778E-01	0.17171E 00
71	0.63922E-02	0.17716E 00
72	0.33521E-01	0.18183E 00
73	0.60565E-01	0.18581E 00
74	0.87428E-01	0.18939E 00
75	0.11411E 00	0.19247E 00
76	0.14052E 00	0.19524E 00
77	0.16664E 00	0.19770E 00
78	0.19239E 00	0.19989E 00
79	0.21772E 00	0.20184E 00
80	0.24257E 00	0.20358E 00
81	0.26684E 00	0.20510E 00
82	0.29047E 00	0.20647E 00
83	0.31337E 00	0.20765E 00
84	0.33544E 00	0.20867E 00
85	0.35660E 00	0.20949E 00
86	0.37672E 00	0.21015E 00
87	0.39582E 00	0.21074E 00
88	0.41396E 00	0.21131E 00
89	0.43138E 00	0.21187E 00

BEST DOCUMENT AVAILABLE

```
 90  0.44814E 00  0.21073E 00
 91  0.46156E 00  0.20281E 00
 92  0.46797E 00  0.19276E 00
 93  0.46992E 00  0.18158E 00
 94  0.46799E 00  0.17112E 00
 95  0.46272E 00  0.16248E 00
 96  0.45668E 00  0.15691E 00
 97  0.44927E 00  0.15345E 00
 98  0.43797E 00  0.15170E 00
```

Case Control Parameters for Flow Solution

```
        SANZ SUPERCRITICAL STATOR HUB SECTION,  FLOW SOLUTION
&PARAMS S=.863,NSTRM=3,RINF=3.724,
MESH1=2,MESHN=4,QUASI3=.TRUE.,
 MS=3,7,13,25,NOZES=-9,-13,-25,-49,
TOLS=1.E04,-2.E-05,
 7.E-05,6.E-05,-.000001,2*0.,
 BETA1=25.1,NOWREL=20,NOTYET=10,
 BETA2=-15.6,LAMDA0=19.5,
 OVEREL=1.6,CII=.4,MINF=.801,
 IT=30,ALLOUT=.TRUE.,SUPREL=2.0,SMOOTH=.TRUE.
RLE=.007,RTE=.029,KN=62,NED=88,CHORD=1.0146
&END
```

Bulk Data Input for Flow Solutions - Stream-Channel Data File

"Streamline number 3" is selected here because NSTRM equals 3 from the case control input.

```
    STREAMLINE NUMBER  1  --  STREAM FUNCTION =  0.0000
  1.40000 1716.4800  581.9998 0.00278050.00061536                    0.000   0.00000
 290.7671    -4.9297  0.119776 0.1001226
   1.0000     0.0010
  21   61              81   20   28   28    1    1    1
0.0013696 0.0038565   54.3510    1.8563   13.0000
 0.000256  0.007862  0.018306  0.028770  0.039246  0.049726  0.060202  0.070664
 0.081105  0.091519  0.101903  0.112255  0.115792
0.0017591 0.0239841 0.0491248 0.0677468 0.0829612 0.0930837 0.0986944 0.1022954
0.1047776 0.1063557 0.1075357 0.1080631 0.1082771
0.0013696 0.0038565   16.9621   -2.6960   13.0000
 0.001768  0.007862  0.018306  0.028770  0.039246  0.049726  0.060202  0.070664
 0.081105  0.091519  0.101903  0.112255  0.115736
-0.0028870 0.0023670 0.0170644 0.0341531 0.0495386 0.0626676 0.0736161 0.0817172
0.0875790 0.0911617 0.0924746 0.0922745 0.0919729
-0.150957 -0.118756 -0.086551 -0.054317 -0.043995 -0.033661 -0.023312 -0.012945
-0.002555  0.007863  0.018306  0.028770  0.039246  0.049726  0.060202  0.070664
 0.081105  0.091519  0.101903  0.112255  0.122580  0.132888  0.143187  0.163188
 0.183188  0.203190  0.223192  0.243194
 0.445770  0.445983  0.446553  0.448051  0.448808  0.449698  0.450734  0.451980
 0.453384  0.454976  0.456732  0.458606  0.460548  0.462512  0.464450  0.466314
 0.468056  0.469629  0.470984  0.472074  0.472866  0.473389  0.473691  0.473822
 0.473641  0.473389  0.473108  0.472820
0.0060057 0.0068080 0.0073119 0.0073806 0.0073717 0.0073965 0.0073621 0.0074961
0.0069645 0.0071813 0.0064250 0.0060114 0.0060900 0.0058698 0.0055669 0.0053046
0.0051044 0.0051718 0.0050349 0.0049574 0.0046936 0.0049132 0.0048774 0.0050551
0.0051724 0.0051911 0.0052327 0.0052886
  0.74436   0.71080   0.69488   0.69051   0.68945   0.68729   0.68636   0.68103
  0.69274   0.74329   0.71332   0.68195   0.56593   0.49017   0.46927   0.46599
  0.47064   0.45210   0.45687   0.47149   0.46048   0.43514   0.43864   0.42024
  0.40927   0.40781   0.40432   0.39965
  0.00000   0.00000   0.00000   0.00000   0.00000   0.00000   0.00000   0.00000
  0.00000   0.00143   0.00333   0.00524   0.00714   0.00905   0.01096   0.01286
  0.01476   0.01666   0.01855   0.02043   0.02180   0.02180   0.02180   0.02180
  0.02180   0.02180   0.02180   0.02180
    1    0    0    2    2    2    3
    STREAMLINE NUMBER  2  --  STREAM FUNCTION =  0.0290
  1.40000 1716.4800  581.7185 0.00300310.00061536                    0.000   0.00000
 299.9548    15.3325  0.120048 0.0929822
   1.0000     0.0010
  21   61              81   20   28   28    1    1    1
0.0015167 0.0038388   53.7777    2.3267   13.0000
 0.000293  0.005101  0.015332  0.025679  0.036083  0.046562  0.057124  0.067719
 0.078345  0.088996  0.099678  0.110391  0.116051
0.0019039 0.0153618 0.0396086 0.0585241 0.0737623 0.0847238 0.0913482 0.0952344
```

BEST DOCUMENT AVAILABLE

```
 0.0977184 0.0990426 0.0999755 0.1004877 0.1008875
 0.0015167 0.0038388   14.8797   -1.8425   13.0000
  0.001904  0.005101  0.015332  0.025679  0.036083  0.046562  0.057124  0.067719
  0.078345  0.088996  0.099678  0.110391  0.116083
-0.0031139-0.0008983 0.0115014 0.0267384 0.0413744 0.0544321 0.0656631 0.0744360
 0.0807123 0.0841923 0.0855135 0.0854021 0.0850744
-0.151271 -0.119060 -0.087167 -0.055544 -0.045453 -0.035364 -0.025275 -0.015178
-0.005052  0.005101  0.015332  0.025679  0.036083  0.046562  0.057124  0.067719
  0.078345  0.088996  0.099678  0.110391  0.12109f  0.131718  0.142263  0.162577
  0.182676  0.202704  0.222718  0.242718
  0.460865  0.462438  0.463745  0.465257  0.465955  0.466842  0.467804  0.469145
  0.469790  0.471835  0.472950  0.473955  0.475829  0.477420  0.478547  0.479806
  0.481111  0.482881  0.484189  0.485120  0.485247  0.486319  0.486553  0.487007
  0.487043  0.486819  0.486621  0.486447
 0.0046231 0.0048699 0.0050106 0.0050022 0.0049897 0.0049849 0.0049670 0.0049825
 0.0048608 0.0050024 0.0049863 0.0048432 0.0049296 0.0047053 0.0046550 0.0042884
 0.0041698 0.0042085 0.0042049 0.0041758 0.0039849 0.0041184 0.0041017 0.0041611
 0.0042039 0.0042081 0.0042270 0.0042528
   0.80177   0.77472   0.76107   0.75856   0.75805   0.75658   0.75593   0.75210
   0.75994   0.79923   0.79827   0.78752   0.69086   0.61466   0.57647   0.55905
   0.55276   0.53098   0.52659   0.53366   0.52112   0.49787   0.50015   0.49051
   0.48419   0.48386   0.48141   0.47797
   0.00000   0.00000   0.00000   0.00000   0.00000   0.00000   0.00000   0.00000
   0.00000   0.00233   0.00707   0.01183   0.01660   0.02140   0.02537   0.02918
   0.03300   0.03790   0.04231   0.04639   0.04869   0.05013   0.04994   0.05082
   0.05139   0.05144   0.05164   0.05192
     1     0     0     2     2     2     3
     STREAMLINE NUMBER  3  --  STREAM FUNCTION =  0.0660
   1.40000 1716.4800  580.3772 0.00307650.00061536                0.000   0.00000
 301.1169   26.5638  0.120740 0.0849164
    1.0000    0.0010
    21    61      81    20    28    28     1     1     1
 0.0015377 0.0038071   52.3556    1.7363   13.0000
  0.000320  0.002507  0.012505  0.022721  0.033036  0.043500  0.054176  0.064928
  0.075749  0.086643  0.097634  0.108728  0.116814
 0.0019246 0.0076624 0.0310414 0.0494432 0.0639724 0.0756444 0.0835645 0.0877343
 0.0901731 0.0912107 0.0917784 0.0921281 0.0925331
 0.0015377 0.0038071   17.2296   -1.8914   12.0000
  0.001992  0.012505  0.022721  0.033036  0.043500  0.054176  0.064928  0.075749
  0.086643  0.097634  0.108728  0.116803
-0.0030097 0.0066846 0.0200145 0.0334604 0.0459736 0.0574908 0.0666530 0.0731229
 0.0765852 0.0780284 0.0777994 0.0773005
-0.151661 -0.119386 -0.087776 -0.056729 -0.046853 -0.036987 -0.027134 -0.017280 }
-0.007403  0.002507  0.012505  0.022721  0.033036  0.043500  0.054176  0.064928 } X array
 0.075749  0.086643  0.097634  0.108728  0.119859  0.130821  0.141635  0.162285 }
 0.182488  0.202545  0.222573  0.242572
 0.477011  0.479328  0.480943  0.482355  0.482990  0.483824  0.484708  0.485999 }
 0.486423  0.488575  0.490045  0.490588  0.492400  0.493683  0.494058  0.494671 } RMSP
 0.495545  0.497453  0.498816  0.499691  0.499553  0.500723  0.500945  0.501510 }
 0.501648  0.501427  0.501281  0.501179
 0.0044123 0.0044123 0.0044123 0.0043910 0.0043778 0.0043678 0.0043544 0.0043436 }
 0.0043085 0.0042972 0.0042854 0.0042799 0.0042605 0.0042533 0.0040468 0.0038859 } BESP
 0.0037686 0.0037823 0.0037835 0.0037555 0.0037736 0.0036978 0.0037031 0.0037062 }
 0.0037222 0.0037203 0.0037305 0.0037453
   0.80894   0.78228   0.77002   0.76917   0.76916   0.76842   0.76795   0.76635
   0.76911   0.79603   0.81327   0.83136   0.75130   0.68170   0.63448   0.60522
   0.59035   0.56646   0.55807   0.56667   0.56089   0.53216   0.53083   0.52955
   0.52646   0.52711   0.52545   0.52292
   0.00000   0.00000   0.00000   0.00000   0.00000   0.00000   0.00000   0.00000
   0.00000   0.00104   0.00495   0.00913   0.01320   0.01750   0.02218   0.02592
   0.02957   0.03411   0.03841   0.04245   0.04553   0.04664   0.04653   0.04710
   0.04751   0.04751   0.04766   0.04788
     1     0     0     2     2     2     3
```

Printed Output List for Flow Solution

```
 QSONIC VERSION 1.5                    SAMZ SUPERCRITICAL STATOR HUB SECTION, FLOW SOLUTION

      CASE CONTROL INPUT ECHO

&PARAMS
NOFLOW= F
RESTAR= F
REMESH= 4
MS= 3, 7, 13, 25, 6*0
NOZES= -9, -13, -25, -49, 6*0
MESH1= 2
MESHN= 4
LAMDA0= 19.50
CHORD= 1.01460
S= 0.8630
NED= 88
KN= 62
RLE= 0.6999999E-02
RTE= 0.290E-01
THETL= 0.0
THETT= 0.0
CAMPER= 6
```

BEST DOCUMENT AVAILABLE

```
 STABAC= 0.9990
 CHOP= 0.9899999
 SMOOTH= T
 LEONLY= F
 SLP1= 1.0
 SLP2= 2.0
 SLP3= 1.0
 SLP4= 1.0
 MINF= 0.8010
 BETA1= 25.09999
 BETA2= -15.60
 GAMMA= 1.40
 TOLS= 10000.0, -0.1999999E-04, 0.6999999E-04, 0.5999999E-04, -0.9999994E-06
 5*0.0
 OVEREL= 1.599999
 UNDERL= 1.0
 SUPREL= 2.0
 NOWREL= 20
 NOTYET= 10
 TEGARD= 2.0
 DAMP= 1.0
 CII= 0.40
 IT= 30
 ALLOUT= T
 QUASI3= T
 NSTPM= 3
 RINF= 3.7240
 WAKE= 0.0
 OMEGA= 0.0
 VAXIAL= 0.0
 FLOCO= 999.0
 MINF2= 10.0
 BIGLAX= F
 &END
```

CALCULATED FLOW PARAMETERS

```
&CONST
CIRCLN= 0.5435562
MINF2= 0.5237770
B2OB1= 0.8488322
R2OR1= 1.050665
RINF= 3.7240
RATLE= 3.810152
&END
```

RELAXATION BEGINS ON GRID OF 7 SURFACE CONTOURS INTERSECTED BY 25 RADIATING LINES

SUPERSONIC RELAXATION PARAMETER, SUPREL= 0.20000E 01

ITERATION COUNT	AVERAGE PHI CORRECTN	RESIDUAL AT T. E.	MAX MACH ON BLADE	CALCULATED CIRCULATION	RELATIVE CIRC ERROR	SUBSONIC RELAX. FAC.	SUPERSONIC RELAX. FAC.
30	0.132439E-02	0.555433E-04	0.125451E 01	0.543548E 00	-0.146940E-04	0.160000E 01	0.200000E 01
60	0.303310E-03	0.295658E-04	0.129494E 01	0.543545E 00	-0.208368E-04	0.160000E 01	0.200000E 01
62	0.277492E-03	0.276545E-04	0.129541E 01	0.543546E 00	-0.186417E-04	0.160000E 01	0.200000E 01

FINAL FLOW CALCULATION ON BLADE SURFACE FOR THE 7 BY 25 MESH

RADIATING LINE NO.	X/CX	Y/CX	X	Y	MACH	STATIC PRES COEF	PHI	XVEL	YVEL	DENSITY
1	0.97785	0.34462	0.44928	0.15345	0.51852	0.48029	0.16124	0.61095	0.23723	1.14972
2	0.91147	0.34329	0.38739	0.15221	0.61619	0.39359	0.10687	0.78732	0.00838	1.12330
3	0.80899	0.34353	0.29187	0.15244	0.49241	0.64894	0.04288	0.63689	0.03868	1.20044
4	0.69078	0.33126	0.18168	0.14108	0.45173	0.72513	-0.02416	0.57863	0.09957	1.22308
5	0.57196	0.30299	0.07092	0.11464	0.44687	0.73392	-0.09013	0.55441	0.17399	1.22568
6	0.45978	0.26005	-0.03365	0.07462	0.45769	0.71476	-0.15576	0.54078	0.24716	1.22001
7	0.35588	0.20590	-0.13051	0.02414	0.48869	0.65755	-0.22207	0.54772	0.31747	1.20301
8	0.26005	0.14617	-0.21983	-0.03153	0.54744	0.54281	-0.29182	0.59204	0.38293	1.16863
9	0.17230	0.08846	-0.30164	-0.08533	0.61931	0.39490	-0.36526	0.66567	0.42804	1.12369
10	0.09589	0.04035	-0.37360	-0.13018	0.67617	0.27331	-0.43604	0.74278	0.42994	1.08622
11	0.03484	0.00815	-0.42977	-0.16019	0.61219	0.39328	-0.49230	0.72736	0.28786	1.12320
12	0.00000	0.00000	-0.46224	-0.16779	0.43585	0.55523	-0.51496	0.36148	0.42995	1.17237
13	0.00192	0.02862	-0.46046	-0.14111	0.72307	0.06974	-0.49851	0.38572	0.82056	1.02227
14	0.04651	0.08636	-0.41889	-0.08728	1.11563	-0.67377	-0.41775	0.88261	0.98542	0.77304
15	0.12651	0.16339	-0.34618	-0.01548	1.29408	-0.99244	-0.26777	1.09891	0.99877	0.65606
16	0.22237	0.24464	-0.25496	0.06026	1.22505	-0.87547	-0.08865	1.14507	0.84663	0.69990
17	0.33046	0.31337	-0.15421	0.12433	1.04750	-0.56195	0.07246	1.11577	0.57814	0.81936
18	0.44444	0.35742	-0.04795	0.16538	0.93431	-0.30100	0.20700	1.09698	0.31918	0.90146
19	0.56086	0.37934	0.06057	0.18582	0.86319	-0.13959	0.33012	1.05532	0.16226	0.95481
20	0.67465	0.39288	0.16664	0.19769	0.78234	0.03996	0.45916	0.97477	0.09298	1.01279
21	0.78214	0.40003	0.26684	0.20511	0.72767	0.16165	0.53332	0.91577	0.05765	1.05134
22	0.87844	0.40474	0.35668	0.20949	0.75593	0.09802	0.61405	0.94878	0.03865	1.03125
23	0.95866	0.40728	0.43138	0.21187	0.63819	0.25368	0.68853	0.78141	-0.20995	1.08012
24	1.00000	0.37480	0.46992	0.18158	0.34361	0.63945	0.72134	0.44473	0.00196	1.19761
25	0.97785	0.34462	0.44928	0.15345	0.51055	0.48027	0.70478	0.61094	0.23736	1.14971

END OF CALCULATION ON GRID 1 OF 3

BEST DOCUMENT AVAILABLE

RELAXATION BEGINS ON GRID OF 13 SURFACE CONTOURS INTERSECTED BY 49 RADIATING LINES

SUPERSONIC RELAXATION PARAMETER, SUPREL= 0.16000E 01

ITERATION COUNT	AVERAGE PHI CORRECTN	RESIDUAL AT T. E.	MAX MACH ON BLADE	CALCULATED CIRCULATION	RELATIVE CIRC ERROR	SUBSONIC RELAX. FAC.	SUPERSONIC RELAX. FAC.
30	0.536023E-03	-0.258415E-04	0.111559E 01	0.543509E 00	-0.872868E-04	0.160000E 01	0.160000E 01
60	0.141884E-03	0.774192E-05	0.113287E 01	0.543546E 00	-0.182038E-04	0.160000E 01	0.160000E 01
90	0.966652E-04	0.729781E-05	0.114052E 01	0.543547E 00	-0.174354E-04	0.160000E 01	0.160000E 01
120	0.727857E-04	0.585704E-05	0.114437E 01	0.543548E 00	-0.154616E-04	0.160000E 01	0.160000E 01
137	0.639313E-04	0.441199E-05	0.114672E 01	0.543549E 00	-0.140361E-04	0.160000E 01	0.160000E 01

FINAL FLOW CALCULATION ON BLADE SURFACE FOR THE 13 BY 49 MESH

RADIATING LINE NO.	X/CX	Y/CX	X	Y	MACH	STATIC PRES COEF	PHI	XVEL	YVEL	DENSITY
1	0.97795	0.34310	0.44928	0.15345	0.78982	-0.04019	0.15487	0.92817	0.32518	0.98707
2	0.95042	0.34133	0.42350	0.15180	0.71379	0.18381	0.12828	0.90083	0.02841	1.05530
3	0.91186	0.34177	0.38739	0.15221	0.58095	0.47438	0.09959	0.74545	-0.01310	1.14793
4	0.86406	0.34291	0.34264	0.15328	0.51288	0.61152	0.06846	0.66288	-0.00317	1.18926
5	0.80983	0.34202	0.29187	0.15244	0.47172	0.68996	0.03645	0.61148	0.02669	1.21265
6	0.75174	0.33791	0.23748	0.14860	0.45030	0.72904	0.00405	0.58220	0.06097	1.22424
7	0.69206	0.32980	0.18160	0.14100	0.44241	0.74316	-0.02851	0.56712	0.09797	1.22841
8	0.63242	0.31763	0.12576	0.12961	0.44194	0.74401	-0.06128	0.55881	0.13522	1.22866
9	0.57385	0.30165	0.07092	0.11464	0.44312	0.74190	-0.09405	0.54991	0.17274	1.22804
10	0.51701	0.28192	0.01770	0.09617	0.44642	0.73607	-0.12663	0.54117	0.21014	1.22631
11	0.46216	0.25890	-0.03365	0.07462	0.45311	0.72415	-0.15922	0.53505	0.24601	1.22279
12	0.40938	0.23310	-0.08308	0.05046	0.46287	0.70651	-0.19199	0.53152	0.28066	1.21756
13	0.35872	0.20499	-0.13051	0.02414	0.47891	0.67697	-0.22507	0.53551	0.31444	1.20879
14	0.31005	0.17550	-0.17608	-0.00347	0.50525	0.62701	-0.25894	0.55266	0.34850	1.19390
15	0.26332	0.14553	-0.21983	-0.03153	0.53928	0.56047	-0.29403	0.58172	0.38067	1.17394
16	0.21849	0.11613	-0.26180	-0.05906	0.57585	0.48657	-0.33010	0.61656	0.40830	1.15163
17	0.17595	0.08807	-0.30164	-0.08533	0.61045	0.41480	-0.36652	0.65401	0.42679	1.12978
18	0.13592	0.06249	-0.33911	-0.10928	0.63735	0.35791	-0.40215	0.63928	0.43079	1.11235
19	0.09908	0.04017	-0.37360	-0.13018	0.61765	0.39878	-0.43549	0.67922	0.40239	1.12488
20	0.06650	0.02150	-0.40411	-0.14766	0.59873	0.43880	-0.46200	0.67744	0.35953	1.13710
21	0.03910	0.00812	-0.42977	-0.16019	0.17308	-0.81450	-0.48418	-0.21084	-0.04639	0.99534
22	0.01825	0.00003	-0.44929	-0.16776	6.22106	-1.54228	-0.48276	6.55885	-0.20155	0.43053
23	0.00441	0.00000	-0.46224	-0.16779	56.36440	-2.22657	-0.62053	4.47947	5.98375	0.00001
24	0.00000	0.00997	-0.46638	-0.15846	6.32647	-1.36754	-0.49262	-2.48300	6.43079	0.50647
25	0.00632	0.02849	-0.46046	-0.14111	0.80365	-0.02053	-0.47991	0.44348	0.89849	0.99340
26	0.02331	0.05436	-0.44455	-0.11689	0.95377	-0.34364	-0.44982	0.78725	0.92268	0.88715
27	0.05072	0.08598	-0.41889	-0.08728	1.08899	-0.61440	-0.39923	0.87627	0.95791	0.79403
28	0.08630	0.12269	-0.38557	-0.05291	1.10408	-0.64386	-0.33654	0.93137	0.92517	0.78364
29	0.12838	0.16267	-0.34618	-0.01548	1.11713	-0.66942	-0.26475	0.97728	0.89504	0.77458
30	0.17532	0.20375	-0.30223	0.02298	1.13097	-0.69652	-0.18676	1.02708	0.85795	0.76493
31	0.22580	0.24357	-0.25496	0.06026	1.14337	-0.72066	-0.10561	1.08273	0.80612	0.75629
32	0.27873	0.28022	-0.20540	0.09458	1.14589	-0.72614	-0.02366	1.13823	0.72986	0.75432
33	0.33341	0.31199	-0.15421	0.12433	1.11188	-0.66160	0.05650	1.16989	0.61119	0.77736
34	0.38953	0.33744	-0.10166	0.14815	1.04958	-0.53805	0.13123	1.17478	0.45944	0.82071
35	0.44689	0.35584	-0.04795	0.16538	0.98921	-0.41184	0.20072	1.15718	0.31549	0.86408
36	0.50494	0.36841	0.00639	0.17716	0.92702	-0.27760	0.26586	1.11526	0.21356	0.90927
37	0.56280	0.37766	0.06057	0.18582	0.87224	-0.15764	0.32627	1.06651	0.15402	0.94890
38	0.61998	0.38477	0.11411	0.19247	0.82790	-0.05995	0.38319	1.02295	0.11649	0.98070
39	0.67608	0.39035	0.16664	0.19769	0.78069	0.04446	0.43622	0.97327	0.08971	1.01422
40	0.73064	0.39478	0.21772	0.20184	0.73919	0.13645	0.48493	0.92802	0.07008	1.04340
41	0.78310	0.39827	0.26684	0.20511	0.71222	0.19585	0.52978	0.89821	0.05561	1.06207
42	0.83280	0.40099	0.31337	0.20765	0.69987	0.22296	0.57121	0.88464	0.04403	1.07054
43	0.87897	0.40295	0.35660	0.20949	0.70178	0.21876	0.60940	0.88730	0.03367	1.06923
44	0.92086	0.40428	0.39582	0.21073	0.75784	0.09340	0.64445	0.95119	0.03089	1.02979
45	0.95884	0.40549	0.43138	0.21187	0.80160	-0.02587	0.68025	0.99022	-0.13275	0.99169
46	0.99107	0.39581	0.46156	0.20281	0.53391	0.40780	0.71232	0.57170	-0.37326	1.12764
47	1.00000	0.37315	0.46992	0.18158	0.12115	0.92023	0.72139	0.15326	-0.04199	1.28029
48	0.99231	0.35274	0.46272	0.16248	0.53366	0.43922	0.71445	0.49221	0.47437	1.13723
49	0.97795	0.34310	0.44928	0.15345	0.78988	-0.04034	0.69762	0.92820	0.32530	0.98702

END OF CALCULATION ON GRID 2 OF 3

RELAXATION BEGINS ON GRID OF 25 SURFACE CONTOURS INTERSECTED BY 97 RADIATING LINES

SUPERSONIC RELAXATION PARAMETER, SUPREL= 0.12000E 01

ITERATION COUNT	AVERAGE PHI CORRECTN	RESIDUAL AT T. E.	MAX MACH ON BLADE	CALCULATED CIRCULATION	RELATIVE CIRC ERROR	SUBSONIC RELAX. FAC.	SUPERSONIC RELAX. FAC.
30	0.158286E-03	-0.831571E-05	0.113079E 01	0.543551E 00	-0.100884E-04	0.160000E 01	0.120000E 01
60	0.635203E-04	0.650720E-06	0.115129E 01	0.543554E 00	-0.405738E-05	0.160000E 01	0.120000E 01
64	0.589319E-04	0.706636E-06	0.115269E 01	0.543555E 00	-0.219314E-05	0.160000E 01	0.120000E 01

FINAL FLOW CALCULATION ON BLADE SURFACE FOR THE 25 BY 97 MESH

RADIATING LINE NO.	X/CX	Y/CX	X	Y	MACH	STATIC PRES COEF	PHI	XVEL	YVEL	DENSITY
1	0.97795	0.34420	0.44928	0.15345	0.96863	-0.38816	0.15264	1.12082	0.35810	0.87212
2	0.96587	0.34232	0.43796	0.15169	0.82943	-0.07382	0.13970	1.02696	0.08536	0.97621
3	0.95043	0.34244	0.42350	0.15180	0.68838	0.26513	0.12618	0.87228	-0.00775	1.07745
4	0.93244	0.34262	0.40666	0.15197	0.61172	0.41198	0.11257	0.78239	-0.00897	1.12889
5	0.91186	0.34287	0.38739	0.15221	0.57356	0.49132	0.09799	0.73662	-0.01340	1.15307
6	0.88898	0.34341	0.36596	0.15271	0.53887	0.56129	0.08263	0.69450	-0.01695	1.17419
7	0.86407	0.34401	0.34264	0.15328	0.50585	0.62598	0.06694	0.65423	-0.00805	1.19357
8	0.83758	0.34399	0.31783	0.15326	0.48168	0.67189	0.05116	0.62435	0.01014	1.20728
9	0.80985	0.34312	0.29187	0.15244	0.46645	0.70018	0.03523	0.60493	0.02688	1.21568
10	0.78114	0.34152	0.26498	0.15094	0.45516	0.72069	0.01913	0.58995	0.04232	1.22176
11	0.75176	0.33902	0.23748	0.14860	0.44655	0.73612	0.00298	0.57761	0.05994	1.22633
12	0.72200	0.33549	0.20961	0.14529	0.44149	0.74512	-0.01320	0.56895	0.07875	1.22899
13	0.69209	0.33090	0.18160	0.14100	0.43979	0.74812	-0.02943	0.56386	0.09766	1.22987
14	0.66219	0.32531	0.15360	0.13576	0.44061	0.74669	-0.04574	0.56132	0.11647	1.22945
15	0.63245	0.31874	0.12576	0.12961	0.44223	0.74381	-0.06214	0.55916	0.13534	1.22860
16	0.60299	0.31121	0.09817	0.12256	0.44269	0.74301	-0.07856	0.55499	0.15370	1.22836
17	0.57389	0.30275	0.07092	0.11464	0.44233	0.74363	-0.09491	0.54911	0.17205	1.22855

BEST DOCUMENT AVAILABLE

18	0.54521	0.29336	0.04407	0.10585	0.44324	0.74201	-0.11119	0.54385	0.19147	1.22887
19	0.51705	0.28302	0.01770	0.09617	0.44585	0.73740	-0.12745	0.54020	0.21069	1.22671
20	0.48938	0.27188	-0.00821	0.08573	0.44919	0.73145	-0.14373	0.53744	0.22854	1.22495
21	0.46221	0.26001	-0.03365	0.07462	0.45313	0.72438	-0.16005	0.53500	0.24619	1.22286
22	0.43556	0.24743	-0.05860	0.06284	0.45765	0.71623	-0.17641	0.53289	0.26372	1.22044
23	0.40942	0.23421	-0.08308	0.05046	0.46303	0.70644	-0.19286	0.53126	0.28168	1.21754
24	0.38387	0.22036	-0.10701	0.03749	0.46961	0.69480	-0.20935	0.53120	0.29829	1.21489
25	0.35877	0.20610	-0.13051	0.02414	0.47723	0.68035	-0.22598	0.53353	0.31371	1.20979
26	0.33419	0.19149	-0.15353	0.01046	0.48892	0.65842	-0.24275	0.54010	0.33091	1.20327
27	0.31010	0.17661	-0.17608	-0.00347	0.50415	0.62947	-0.25983	0.55139	0.34831	1.19463
28	0.28668	0.16166	-0.19820	-0.01747	0.52141	0.59602	-0.27721	0.56519	0.36606	1.18462
29	0.26338	0.14664	-0.21983	-0.03153	0.54007	0.55922	-0.29492	0.58166	0.38254	1.17357
30	0.24068	0.13180	-0.24108	-0.04543	0.55823	0.52281	-0.31294	0.59918	0.39603	1.16259
31	0.21856	0.11725	-0.26180	-0.05906	0.57584	0.48692	-0.33105	0.61621	0.40883	1.15173
32	0.19699	0.10301	-0.28200	-0.07239	0.59434	0.44869	-0.34924	0.63475	0.42108	1.14012
33	0.17601	0.08919	-0.30164	-0.08533	0.61222	0.41132	-0.36745	0.65500	0.42912	1.12872
34	0.15565	0.07606	-0.32071	-0.09763	0.62731	0.37943	-0.38547	0.67398	0.43278	1.11895
35	0.13599	0.06361	-0 33911	-0.10928	0.63971	0.35300	-0.40312	0.69082	0.43357	1.11084
36	0.11713	0.95198	-0.35678	-0.12018	0.64771	0.33590	-0.42020	0.70492	0.42867	1.10557
37	0.09916	0.04129	-0.37360	-0.13018	0.65213	0.32646	-0.43643	0.71447	0.42286	1.10266
38	0.08226	0.03142	-0.38943	-0.13943	0.65852	0.31265	-0.45170	0.72635	0.41732	1.09840
39	0.06658	0.02262	-0.40411	-0.14766	0.65601	0.31770	-0.46598	0.73689	0.39215	1.09996
40	0.05204	0.01535	-0.41773	-0.15448	0.64073	0.35074	-0.47850	0.73385	0.35864	1.11014
41	0.03918	0.00924	-0.42977	-0.16019	0.61664	0.40173	-0.48926	0.71538	0.33129	1.12579
42	0.02795	0.00420	-0.44028	-0.16492	0.60532	0.42378	-0.49813	0.72395	0.27592	1.13250
43	0.01833	0.00116	-0.44929	-0.16776	0.51533	0.59251	-0.50552	0.64624	0.15868	1.18357
44	0.01053	0.00000	-0.45659	-0.16885	0.48030	0.80584	-0.50959	0.52226	-0.88576	1.24687
45	0.00449	0.00113	-0.46224	-0.16779	0.22327	0.99709	-0.51249	0.28446	-0.07376	1.30255
46	0.00000	0.00457	-0.46645	-0.16457	0.63265	-0.14069	-0.51296	0.04558	0.78117	0.95445
47	0.00008	0.01109	-0.46638	-0.15846	0.94629	-0.40124	-0.50322	0.09148	1.14467	0.86768
48	0.00209	0.01938	-0.46450	-0.15070	0.69524	0.20361	-0.49804	0.28935	0.82988	1.06450
49	0.00640	0.02962	-0.46046	-0.14111	0.94703	-0.32675	-0.48689	0.52484	1.02978	0.89283
50	0.01355	0.04171	-0.45376	-0.12979	1.07474	-0.58740	-0.47050	0.78168	1.07568	0.80351
51	0.02339	0.05548	-0.44455	-0.11689	1.12790	-0.69157	-0.44948	0.81752	1.05573	0.76670
52	0.03598	0.07048	-0.43276	-0.10285	1.13641	-0.70652	-0.42476	0.87787	1.01695	0.76135
53	0.05079	0.08710	-0.41889	-0.08728	1.12764	-0.68966	-0.39678	0.90269	0.98388	0.76738
54	0.06766	0.10486	-0.40310	-0.07065	1.11558	-0.66606	-0.36622	0.91955	0.95228	0.77578
55	0.08638	0.12381	-0.38557	-0.05291	1.10170	-0.63886	-0.33333	0.92922	0.92416	0.78541
56	0.10669	0.14351	-0.36655	-0.03447	1.08801	-0.61174	-0.29870	0.93843	0.89587	0.79497
57	0.12845	0.16378	-0.34618	-0.01548	1.08058	-0.59698	-0.26269	0.95013	0.87287	0.80018
58	0.15137	0..8436	-0.32471	0.00379	1.08532	-0.60663	-0.22568	0.97219	0.85518	0.79684
59	0.17538	0.20486	-0.30223	0.02298	1.09802	-0.62768	-0.18689	1.00111	0.83728	0.78936
60	0.20027	0.22504	-0.27893	0.04187	1.10699	-0.64932	-0.14749	1.03064	0.81765	0.78171
61	0.22586	0.24467	-0.25496	0.06026	1.12032	-0.67543	-0.10758	1.06332	0.79601	0.77244
62	0.25206	0.26355	-0.23043	0.07793	1.13612	-0.70611	-0.06701	1.10140	0.76874	0.76150
63	0.27879	0.28133	-0.20540	0.09458	1.14889	-0.73059	-0.02629	1.13983	0.73287	0.75272
64	0.30594	0.29789	-0.17998	0.11009	1.15275	-0.73801	0.01431	1.17189	0.68755	0.75006
65	0.33346	0.31309	-0.15421	0.12433	1.13542	-0.70506	0.05448	1.18752	0.62610	0.76188
66	0.36132	0.32677	-0.12812	0.13713	1.08646	-0.60976	0.09306	1.17751	0.54082	0.79567
67	0.38958	0.33854	-0.10166	0.14815	1.03567	-0.50682	0.12939	1.16204	0.45002	0.83153
68	0.41816	0.34850	-0.07490	0.15748	1.02044	-0.47504	0.16424	1.17095	0.37988	0.84248
69	0.44694	0.35694	-0.04795	0.16538	1.00824	-0.44991	0.19895	1.17768	0.31386	0.85109
70	0.47596	0.36370	-0.02078	0.17171	0.96416	-0.35661	0.23255	1.14668	0.25205	0.88278
71	0.50498	0.36951	0.00639	0.17716	0.92239	-0.26664	0.26429	1.11112	0.20986	0.91292
72	0.53395	0.37450	0.03352	0.18183	0.89571	-0.20867	0.29505	1.08841	0.17649	0.93212
73	0.56283	0.37876	0.06057	0.18582	0.87026	-0.15290	0.32481	1.06477	0.15144	0.95045
74	0.59152	0.38258	0.08743	0.18939	0.85024	-0.10888	0.35362	1.04562	0.13189	0.96482
75	0.62001	0.38587	0.11411	0.19267	0.83132	-0.06712	0.38169	1.02689	0.11512	0.97837
76	0.64822	0.38883	0.14053	0.19525	0.80632	-0.01193	0.40883	1.00076	0.10121	0.99617
77	0.67611	0.39145	0.16664	0.19749	0.77829	0.05010	0.43480	0.97071	0.08857	1.01602
78	0.70361	0.39380	0.19239	0.19990	0.75379	0.10432	0.45960	0.94401	0.07814	1.03325
79	0.73066	0.39588	0.21772	0.20184	0.73455	0.14681	0.48337	0.92286	0.06904	1.04666
80	0.75720	0.39773	0.24257	0.20358	0.71929	0.18040	0.50618	0.90596	0.06141	1.05722
81	0.78312	0.39936	0.26684	0.20511	0.70721	0.20691	0.52807	0.89250	0.05492	1.06553
82	0.80836	0.40081	0.29047	0.20646	0.69873	0.22546	0.54910	0.88305	0.04933	1.07133
83	0.83281	0.40208	0.31337	0.20765	0.69455	0.23459	0.56929	0.87851	0.04394	1.07417
84	0.85639	0.40317	0.33545	0.20867	0.69350	0.23689	0.58871	0.87756	0.03820	1.07489
85	0.87898	0.40405	0.35660	0.20949	0.69424	0.23527	0.60731	0.87866	0.03228	1.07438
86	0.90046	0.40475	0.37672	0.21015	0.69751	0.22814	0.62502	0.88256	0.02853	1.07216
87	0.92086	0.40537	0.39582	0.21073	0.70946	0.20192	0.64195	0.89631	0.02866	1.06397
88	0.94023	0.40599	0.41396	0.21131	0.75597	0.09853	0.65842	0.94914	0.03092	1.05141
89	0.95884	0.40658	0.43138	0.21187	0.90415	-0.23525	0.67578	1.11060	-0.02671	0.92534
90	0.97674	0.40537	0.44814	0.21073	0.91662	-0.31289	0.69630	1.07323	-0.31976	0.89748
91	0.99107	0.39691	0.46156	0.20281	0.65316	0.25183	0.71300	0.62451	-0.54368	1.07954
92	0.99791	0.38618	0.46797	0.19276	0.30668	0.89273	0.72050	0.18193	-0.35822	1.27229
93	1.00000	0.37424	0.46992	0.18158	0.04073	1.10174	0.72230	0.03883	0.03732	1.33261
94	0.99796	0.36307	0.46799	0.17112	0.31964	0.90129	0.71992	0.17354	0.38127	1.27478
95	0.99231	0.35384	0.46272	0.16248	0.57935	0.44651	0.71398	0.48180	0.56485	1.13945
96	0.98586	0.34790	0.45668	0.15691	0.86411	-0.17413	0.70642	0.89370	0.58167	0.94349
97	0.97795	0.34420	0.44928	0.15345	0.96866	-0.38822	0.69619	1.12084	0.35814	0.87210

END OF CALCULATION ON GRID 3 OF 3

CALCULATED FLOW FIELD AT ALL GRID POINTS

SURFACE CONTOUR NO. 1 = PERIODIC BOUNDARY
SURFACE CONTOUR NO. 25 = BLADE SURFACE

RADIATING LINE NO. 1 BEGINS AT DOWNSTREAM INFINITY
AND IS REPEATED AS LINE NO. 97

	SURFACE CONTOUR NUMBER	X/CX	Y/CX	PHI	XVEL	YVEL	DENSITY	MACH	FLOW ANGLE	STATIC PRES COEF
RADIATING LINE NUMBER 1										
	1	2.61888	0.28848	1.48505	-0.24396	0.43447	0.51703	0.52378	119.31493	-1.55813
	2	1.79453	0.28823	0.93527	1.34087	-0.27375	0.61525	0.52378	-11.53872	3.77358
	3	1.59681	0.28861	0.53292	0.68003	0.04605	1.18072	0.52378	3.87384	0.62970
	4	1.48079	0.28922	0.45907	0.68019	0.04635	1.18063	0.52825	3.89807	0.58273
	5	1.39876	0.28985	0.40689	0.67974	0.04673	1.18084	0.52791	3.93293	0.58341
	6	1.33567	0.29064	0.36680	0.67831	0.04734	1.18150	0.52678	3.99231	0.58563
	7	1.28475	0.29159	0.33455	0.67569	0.04828	1.18273	0.52469	4.08721	0.58971
	8	1.24228	0.29272	0.30780	0.67214	0.04969	1.18438	0.52189	4.22799	0.59528
	9	1.20611	0.29404	0.28516	0.66779	0.05172	1.18637	0.51848	4.42886	0.60185
	10	1.17482	0.29554	0.26574	0.66274	0.05462	1.18865	0.51456	4.71101	0.60946
	11	1.14747	0.29721	0.24892	0.65708	0.05866	1.19114	0.51025	5.10144	0.61779

BEST DOCUMENT AVAILABLE

12	1.12338	0.29989	0.23427	0.65087	0.06422	1.19378	0.58564	5.63477	0.62663
13	1.10202	0.30116	0.22146	0.64413	0.07179	1.19652	0.58085	6.35969	0.63580
14	1.08306	0.30344	0.21024	0.63660	0.08173	1.19961	0.49574	7.31591	0.64548
15	1.06616	0.30592	0.20043	0.62887	0.09462	1.20288	0.49098	8.55638	0.65444
16	1.05111	0.30862	0.19187	0.62294	0.11116	1.20349	0.48843	10.11721	0.65917
17	1.03774	0.31153	0.18443	0.62088	0.13178	1.20257	0.48999	11.98352	0.65608
18	1.02588	0.31468	0.17796	0.62470	0.15684	1.19820	0.49759	14.09324	0.64143
19	1.01543	0.31806	0.17235	0.63717	0.18630	1.18885	0.51366	16.29849	0.61013
20	1.00629	0.32170	0.16752	0.66185	0.21954	1.17247	0.54105	18.35106	0.55558
21	0.99839	0.32559	0.16338	0.70310	0.25508	1.14661	0.58295	19.94038	0.46939
22	0.99164	0.32976	0.15985	0.76585	0.29024	1.10734	0.64278	20.75589	0.34162
23	0.98601	0.33421	0.15689	0.85451	0.32104	1.05156	0.72386	20.59146	0.16237
24	0.98146	0.33896	0.15445	0.97207	0.34396	0.97523	0.83009	19.48599	-0.07682
25	0.97795	0.34420	0.15264	1.12082	0.35810	0.87212	0.96863	17.71860	-0.38816

RADIATING LINE NUMBER 2

1	1.64542	-0.16594	0.53726	0.12880	1.54987	0.84221	0.52378	85.24683	8.36990
2	1.59934	-0.00776	0.61053	1.01730	0.15876	0.91636	0.52378	8.86996	2.83198
3	1.51437	0.09003	0.47147	0.68114	0.04697	1.18015	0.52378	3.94507	0.63811
4	1.43474	0.14504	0.42317	0.68186	0.04860	1.17975	0.52975	4.07679	0.57978
5	1.36799	0.17852	0.38213	0.68149	0.04968	1.17989	0.52951	4.16959	0.58026
6	1.31253	0.20088	0.34783	0.68026	0.05104	1.18043	0.52859	4.29849	0.58206
7	1.26578	0.21705	0.31890	0.67817	0.05283	1.18137	0.52700	4.45435	0.58520
8	1.22582	0.22949	0.29422	0.67545	0.05518	1.18259	0.52493	4.67074	0.58924
9	1.19124	0.23957	0.27295	0.67228	0.05822	1.18398	0.52256	4.94971	0.59388
10	1.16181	0.24813	0.25446	0.66884	0.06214	1.18545	0.52005	5.30828	0.59877
11	1.13437	0.25563	0.23828	0.66530	0.06717	1.18689	0.51757	5.76485	0.60359
12	1.11076	0.26242	0.22407	0.66174	0.07362	1.18824	0.51524	6.34819	0.60811
13	1.08974	0.26876	0.21155	0.65797	0.08168	1.18957	0.51295	7.07634	0.61253
14	1.07099	0.27477	0.20052	0.65420	0.09146	1.19072	0.51096	7.95851	0.61637
15	1.05425	0.28059	0.19083	0.65186	0.10337	1.19097	0.51051	9.01066	0.61721
16	1.03931	0.28631	0.18231	0.65289	0.11752	1.18936	0.51325	10.20358	0.61183
17	1.02598	0.29200	0.17482	0.65892	0.13361	1.18507	0.52056	11.46280	0.59752
18	1.01416	0.29773	0.16824	0.67174	0.15105	1.17721	0.53379	12.67282	0.57132
19	1.00371	0.30353	0.16245	0.69345	0.16863	1.16467	0.55447	13.66786	0.52970
20	0.99455	0.30946	0.15736	0.72602	0.18424	1.14640	0.58380	14.23914	0.46934
21	0.98660	0.31555	0.15287	0.77070	0.19466	1.12161	0.62227	14.17534	0.38809
22	0.97981	0.32185	0.14891	0.82697	0.19567	1.09039	0.66901	13.31188	0.28675
23	0.97412	0.32838	0.14542	0.89162	0.18294	1.05416	0.72142	11.59487	0.17063
24	0.96949	0.33519	0.14235	0.95849	0.15461	1.01579	0.77525	9.16329	0.04937
25	0.96587	0.34232	0.13970	1.02698	0.08536	0.97621	0.82943	4.75160	-0.07382

RADIATING LINE NUMBER 3

1	1.44305	-0.16667	0.41391	0.68296	0.04555	1.17932	0.52378	3.81530	0.65056
2	1.42930	-0.07841	0.40905	0.68316	0.04679	1.17918	0.52378	3.91844	0.65258
3	1.39537	-0.00340	0.39092	0.68444	0.04876	1.17849	0.52378	4.07482	0.66280
4	1.35250	0.05440	0.36620	0.68520	0.05066	1.17806	0.53260	4.22870	0.57415
5	1.30852	0.09748	0.34011	0.68479	0.05230	1.17820	0.53236	4.36772	0.57462
6	1.26704	0.13003	0.31520	0.68374	0.05435	1.17863	0.53164	4.54491	0.57606
7	1.22922	0.15525	0.29236	0.68220	0.05686	1.17927	0.53055	4.76461	0.57820
8	1.19517	0.17541	0.27177	0.68035	0.05991	1.18004	0.52925	5.03197	0.58074
9	1.16463	0.19204	0.25333	0.67839	0.06358	1.18082	0.52792	5.35456	0.58336
10	1.13724	0.20618	0.23685	0.67647	0.06802	1.18154	0.52671	5.74230	0.58573
11	1.11265	0.21852	0.22213	0.67465	0.07340	1.18213	0.52569	6.20898	0.58773
12	1.09057	0.22954	0.20900	0.67269	0.07974	1.18272	0.52469	6.76014	0.58970
13	1.07071	0.23960	0.19738	0.67067	0.08697	1.18326	0.52377	7.38871	0.59149
14	1.05285	0.24898	0.18691	0.66969	0.09524	1.18319	0.52389	8.09408	0.59124
15	1.03678	0.25785	0.17767	0.67126	0.10451	1.18178	0.52628	8.84960	0.58653
16	1.02235	0.26637	0.16946	0.67663	0.11425	1.17845	0.53189	9.58398	0.57545
17	1.00944	0.27467	0.16216	0.68687	0.12373	1.17269	0.54151	10.21190	0.55629
18	0.99793	0.28285	0.15566	0.70296	0.13185	1.16404	0.55575	10.62161	0.52761
19	0.98773	0.29098	0.14987	0.72539	0.13687	1.15228	0.57476	10.68520	0.48872
20	0.97876	0.29914	0.14469	0.75360	0.13663	1.13768	0.59785	10.27616	0.44070
21	0.97096	0.30740	0.14005	0.78567	0.12868	1.12123	0.62327	9.30144	0.38687
22	0.96427	0.31580	0.13591	0.81808	0.11111	1.10471	0.64825	7.73454	0.33311
23	0.95863	0.32440	0.13223	0.84609	0.08353	1.09051	0.66931	5.63855	0.28716
24	0.95405	0.33322	0.12901	0.86499	0.04743	1.08098	0.68318	3.13842	0.25646
25	0.95043	0.34244	0.12618	0.87228	-0.00775	1.07745	0.68838	-0.50906	0.24513

RADIATING LINE NUMBER 4

1	1.32347	-0.16789	0.33715	0.68865	0.04496	1.17657	0.53589	3.73567	0.56921
2	1.31638	-0.10591	0.33533	0.68897	0.04753	1.17633	0.53558	3.94673	0.56841
3	1.29861	-0.04851	0.32653	0.68975	0.05005	1.17587	0.53628	4.15022	0.56687
4	1.27354	0.00144	0.31278	0.68989	0.05213	1.17572	0.53652	4.32100	0.56638
5	1.24479	0.04340	0.29635	0.68950	0.05454	1.17583	0.53635	4.52247	0.56672
6	1.21505	0.07816	0.27902	0.68873	0.05725	1.17609	0.53591	4.75160	0.56760
7	1.18592	0.10704	0.26188	0.68774	0.06029	1.17644	0.53531	5.01013	0.56877
8	1.15829	0.13131	0.24554	0.68668	0.06375	1.17681	0.53470	5.30383	0.56999
9	1.13249	0.15201	0.23027	0.68560	0.06770	1.17715	0.53355	5.61652	0.57227
10	1.10864	0.17001	0.21618	0.68444	0.07214	1.17749	0.53280	5.93398	0.57376
11	1.08674	0.18592	0.20327	0.68298	0.07702	1.17794	0.53188	6.88588	0.57557
12	1.06669	0.20026	0.19154	0.68124	0.08227	1.17848	0.53155	7.36506	0.57621
13	1.04839	0.21337	0.18094	0.68014	0.08791	1.17868	0.53277	7.84161	0.57381
14	1.03175	0.22555	0.17139	0.68085	0.09377	1.17795	0.53277	8.26717	0.56788
15	1.01662	0.23705	0.16279	0.68427	0.09942	1.17591	0.53620	8.57999	0.55482
16	1.00293	0.24804	0.15504	0.69108	0.10427	1.17224	0.54231	8.71283	0.53672
17	0.99058	0.25866	0.14806	0.70167	0.10752	1.16679	0.55132	8.71283	0.51312
18	0.97950	0.26904	0.14176	0.71584	0.10811	1.15946	0.56294	8.58797	0.48562
19	0.96961	0.27928	0.13607	0.73270	0.10478	1.15134	0.57638	8.13810	0.45688
20	0.96085	0.28948	0.13094	0.75063	0.09643	1.14281	0.59025	7.32026	0.43045
21	0.95317	0.29971	0.12632	0.76747	0.08245	1.13456	0.60287	6.13171	0.41007
22	0.94653	0.31005	0.12219	0.78083	0.06307	1.12834	0.61251	4.61824	0.39901
23	0.94089	0.32058	0.11853	0.78855	0.03960	1.12496	0.61771	2.87468	0.39901
24	0.93628	0.33112	0.11538	0.78933	0.01385	1.12501	0.61763	1.00589	0.39918
25	0.93244	0.34262	0.11257	0.78239	-0.00897	1.12889	0.61172	-0.65681	0.41190

RADIATING LINE NUMBER 5

1	1.23705	-0.16958	0.28106	0.69605	0.04466	1.17296	0.54114	3.67128	0.55719
2	1.23228	-0.12090	0.28010	0.69626	0.04758	1.17276	0.54147	3.90938	0.55654
3	1.22100	-0.07425	0.27494	0.69631	0.05064	1.17263	0.54169	4.15975	0.55611
4	1.20457	-0.03131	0.26638	0.69610	0.05360	1.17263	0.54178	4.40347	0.55609
5	1.18468	0.00710	0.25545	0.69568	0.05665	1.17271	0.54155	4.65500	0.55638
6	1.16294	0.04093	0.24318	0.69508	0.05986	1.17288	0.54128	4.92174	0.55692
7	1.14056	0.07054	0.23037	0.69431	0.06325	1.17311	0.54090	5.20551	0.55768
8	1.11839	0.09648	0.21757	0.69332	0.06685	1.17342	0.54036	5.50717	0.55874
9	1.09696	0.11937	0.20516	0.69192	0.07062	1.17393	0.53952	5.82792	0.56042
10	1.07660	0.13976	0.19338	0.69002	0.07449	1.17466	0.53831	6.16144	0.56284
11	1.05745	0.15814	0.18236	0.68780	0.07839	1.17553	0.53684	6.50234	0.56574

BEST DOCUMENT AVAILABLE

	12	1.03957	0.17489	0.17214	0.68595	0.08232	1.17621	0.53571	6.84326	0.56888
	13	1.02302	0.19038	0.16277	0.68546	0.08613	1.17622	0.53570	7.16189	0.56802
	14	1.00773	0.20485	0.15416	0.68708	0.08947	1.17526	0.53730	7.42036	0.56485
	15	0.99369	0.21853	0.14629	0.69094	0.09195	1.17318	0.54077	7.58837	0.55794
	16	0.98085	0.23162	0.13911	0.69734	0.09304	1.16997	0.54611	7.59977	0.54726
	17	0.96916	0.24426	0.13254	0.70577	0.09209	1.16586	0.55288	7.43403	0.53363
	18	0.95858	0.25659	0.12655	0.71541	0.08843	1.16126	0.56039	7.04627	0.51862
	19	0.94905	0.26872	0.12108	0.72521	0.08153	1.15671	0.56778	6.41471	0.50335
	20	0.94055	0.28077	0.11613	0.73485	0.07125	1.15272	0.57418	5.54387	0.49020
	21	0.93301	0.29281	0.11165	0.74076	0.05777	1.14986	0.57876	4.45901	0.48074
	22	0.92641	0.30493	0.10762	0.74442	0.04170	1.14849	0.58091	3.20631	0.47625
	23	0.92073	0.31719	0.10403	0.74466	0.02489	1.14876	0.58046	1.85278	0.47714
	24	0.91601	0.32943	0.10091	0.74179	0.00578	1.15043	0.57777	0.44628	0.48263
	25	0.91186	0.34287	0.09799	0.73662	-0.01340	1.15387	0.57356	-1.04241	0.49132
RADIATING LINE NUMBER 6										
	1	1.16846	-0.17173	0.23682	0.70453	0.04465	1.16877	0.54818	3.62688	0.54329
	2	1.16468	-0.13088	0.23528	0.70441	0.04816	1.16872	0.54818	3.91897	0.54311
	3	1.15641	-0.09105	0.23179	0.70484	0.05187	1.16877	0.54810	4.21344	0.54329
	4	1.14453	-0.05328	0.22598	0.70345	0.05543	1.16883	0.54783	4.50516	0.54382
	5	1.12985	-0.01823	0.21815	0.70259	0.05892	1.16921	0.54737	4.79367	0.54475
	6	1.11331	0.01383	0.20913	0.70138	0.06241	1.16966	0.54662	5.08508	0.54625
	7	1.09573	0.04292	0.19936	0.69972	0.06588	1.17033	0.54552	5.37895	0.54847
	8	1.07778	0.06926	0.18930	0.69748	0.06930	1.17127	0.54396	5.67431	0.55158
	9	1.05996	0.09316	0.17930	0.69468	0.07260	1.17248	0.54194	5.96613	0.55561
	10	1.04261	0.11493	0.16957	0.69172	0.07575	1.17376	0.53988	6.24916	0.55987
	11	1.02595	0.13491	0.16028	0.68920	0.07875	1.17483	0.53802	6.51892	0.56341
	12	1.01014	0.15340	0.15151	0.68784	0.08151	1.17533	0.53718	6.75773	0.56509
	13	0.99526	0.17066	0.14330	0.68807	0.08371	1.17510	0.53758	6.93662	0.56429
	14	0.98134	0.18692	0.13564	0.69002	0.08515	1.17406	0.53931	7.03454	0.56085
	15	0.96841	0.20240	0.12852	0.69350	0.08543	1.17234	0.54218	7.02258	0.55514
	16	0.95644	0.21725	0.12192	0.69804	0.08414	1.17019	0.54575	6.87337	0.54799
	17	0.94544	0.23163	0.11583	0.70301	0.08095	1.16791	0.54958	6.56869	0.54044
	18	0.93539	0.24567	0.11023	0.70778	0.07561	1.16583	0.55293	6.09720	0.53354
	19	0.92625	0.25948	0.10508	0.71173	0.06799	1.16423	0.55554	5.45715	0.52825
	20	0.91800	0.27318	0.10038	0.71422	0.05822	1.16341	0.55687	4.65588	0.52558
	21	0.91060	0.28686	0.09610	0.71472	0.04652	1.16357	0.55658	3.72369	0.52605
	22	0.90404	0.30062	0.09223	0.71295	0.03330	1.16481	0.55452	2.67436	0.53016
	23	0.89836	0.31431	0.08876	0.70894	0.01904	1.16706	0.55078	1.53863	0.53762
	24	0.89336	0.32847	0.08560	0.70273	0.00362	1.17025	0.54547	0.29535	0.54818
	25	0.88898	0.34341	0.08263	0.69450	-0.01695	1.17419	0.53887	-1.39848	0.56129

OUTPUT continues for all 97 radiating lines

Plot Output

The graphic output (figs. 9 to 15) was produced by a local graphics package at Lewis, by using the plot data save file.

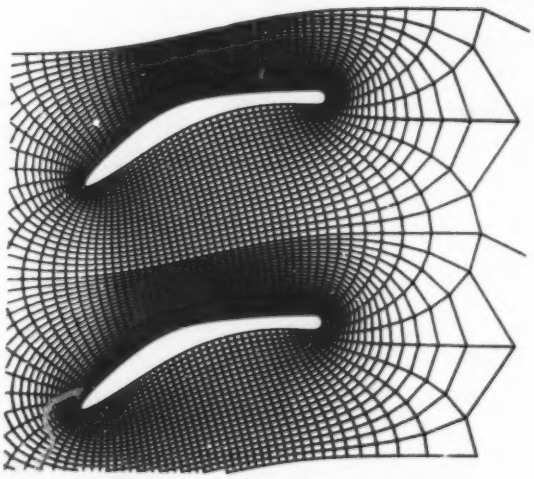

Figure 9. - Solution mesh.

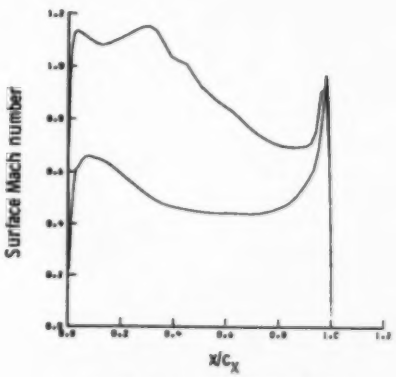

Figure 10. - Surface Mach number.

BEST DOCUMENT AVAILABLE

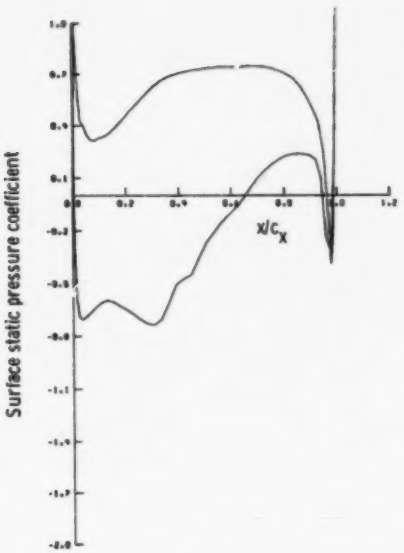

Figure 11. - Surface static pressure.

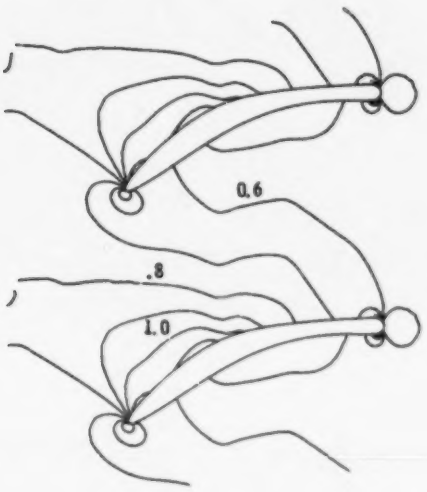

Figure 12. - Isomachs.

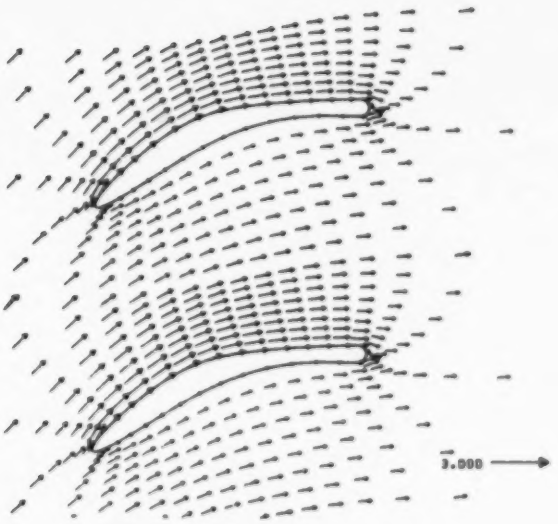

Figure 13. - Velocity vector field.

BEST DOCUMENT AVAILABLE

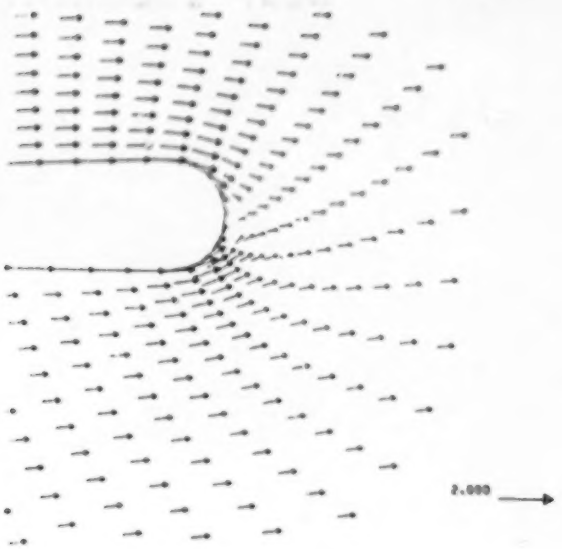

Figure 15. - Trailing-edge region.

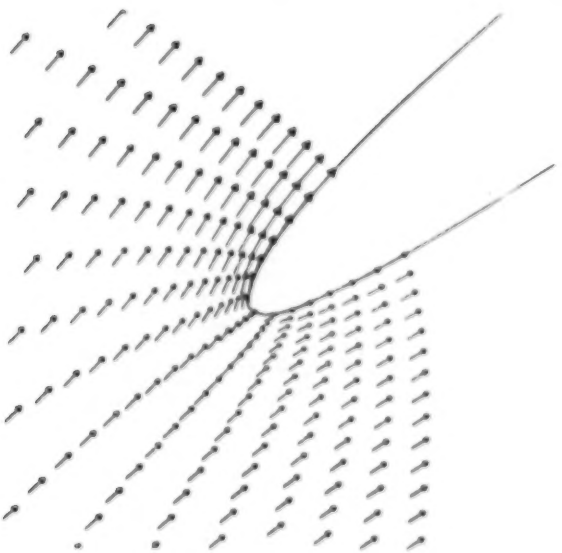

Figure 14. - Leading-edge region.

Lewis Research Center
National Aeronautics and Space Administration
Cleveland, Ohio, Dec. 11, 1981

BEST DOCUMENT AVAILABLE

APPENDIX - SYMBOLS

A	variable coefficient of change in potential for field equation (eqs. (19), (21)); flow area normal to stream-channel direction (eqs. (26) to (31))
A_E	total surface area of finite volume element
a	contravariant velocity component (η direction) in computational space
b	contravariant velocity component (ζ direction) in computational space
C	circulation about airfoil as defined by given values of flow angle
c	blade chord
c_x	length of passage along x axis, from leading edge to trailing edge when blade is at setting angle
e_x, e_y	direction cosines, defined in eq. (15)
G	transposed terms in field equation involving known (previously determined) potential corrections
h	local stream-tube height normalized to unity far upstream
ℓ	length of bounding surfaces for finite volume (fig. 4)
M	Mach number relative to blade
$\hat{n}$	unit vector, normal to airfoil surface in eq. (34); normal to faces of finite volume in eqs. (4), (5), and (7)
q	magnitude of flow speed, normalized to unity at far upstream conditions
R	residual net mass flow out of a finite volume calculated by using potential values from previous iteration (eq. (6) or (16))
δR	change in net mass flow out of a volume caused by changes $\delta\varphi$ in potential values
$\mathscr{R}$	total residual right side for field equation at each volume, $-R + G$
r	local spanwise radial position of stream channel normalized to unity far upstream
S	flow direction as defined by contravariant velocities a and b in eq. (24)
s	blade spacings

BEST DOCUMENT AVAILABLE

u	x component of relative velocity in physical plane
δu	change in relative streamwise velocity caused by changes $\delta\varphi$
V	total absolute velocity vector, $u\hat{i} + v\hat{j} + \Omega r\hat{j}$
$\mathcal{V}$	volume of element surrounding a grid point; equals area of element within stream surface times stream-channel thickness
v	y component of relative velocity in physical plane
δv	change in relative tangential velocity caused by changes $\delta\varphi$
W	total relative velocity vector, $u\hat{i} + v\hat{j}$
δW	change in total relative velocity caused by changes $\delta\varphi$
x	position coordinate along stream channel (fig. 1)
y	tangential position coordinate (fig. 1) = $r_{LE} \cdot \theta$
α	angle of flow as measured from x axis
β	angle of flow as measured from chordline
γ	ratio of specific heats
ζ	coordinate in computational space whose contours in physical space radiate from blade and terminate on periodic boundary
η	coordinate in computational space whose physical contours surround airfoil
θ	tangential coordinate in radians, $y = \theta \cdot r_{LE}$
λ	stagger or setting angle of blade row, as measured from x axis to chordline
μ	switch function to control artificial density modification (eq. (23))
π	3.14159265
ρ	physical density
$\delta\rho$	change in physical density caused by changes $\delta\varphi$
$\tilde{\rho}$	artificial density as described in eq. (22)
φ	flow velocity potential function
$\delta\varphi$	change in local potential field; unknowns in eq. (14)

BEST DOCUMENT AVAILABLE

Ω	angular velocity of blade row, rad/sec
ω	overrelaxation parameter, $1 < \omega < 2$

Subscripts:

a	absolute frame of reference fixed in space
av	average
i	position on computational plane in ξ direction
j	position on computational plane in η direction
LE	at leading edge of blade
ξ	differentiation with respect to ξ
η	differentiation with respect to η
in	conditions at far upstream station
out	conditions at far downstream station

Superscripts:

k,K	artificial time step (iteration level)
$(\bar{\ })$	average over the length Δ of velocity component normal to element surface along Δ (eq. (16) and fig. 4)

BEST DOCUMENT AVAILABLE

REFERENCES

1. Hafez, M.; South, J.; and Murman, E.: Artificial Compressibility Methods for Numerical Solutions of Transonic Full Potential Equation. AIAA Journal, vol. 17, no. 8, Aug. 1979, pp. 838-844.

2. Katsanis, Theodore: FORTRAN Program for Calculating Transonic Velocities on a Blade-to-Blade Stream Surface of a Turbomachine. NASA TN D-5427, 1969.

3. Farrell, C.; and Adamczyk, J.: Full Potential Solution of Transonic Quasi-3-D Flow Through a Cascade Using Artificial Compressibility. ASME Paper 81-GT-70, Mar. 1981.

4. Caughey, D. A.; and Jameson, A.: Numerical Calculation of Transonic Potential Flow About Wing-Fuselage Combinations. AIAA Paper 77-677, June 1977.

5. Casper, J. R.; Hobbs, D. E.; and Davis, R. L.: The Calculation of Potential Flow in Cascades Using Finite Area Techniques. AIAA Paper 79-0077, Jan. 1979.

6. Roache, Patrick J.: Computational Fluid Dynamics. Rev. printing. Hermosa Publishers, 1976, pp. 345-349.

7. Forsythe, George E.; and Moler, Cleve B.: Computer Solutions of Linear Algebraic Systems. Prentice-Hall, 1967.

8. Bauer, Frances; et al.: Supercritical Wing Sections II; a Handbook. Lecture Notes in Economics and Mathematical Systems, Vol. 108: Control Theory, Springer-Verlag, 1975.

BEST DOCUMENT AVAILABLE

1. Report No. NASA TP-2030	2. Government Accession No.	3. Recipient's Catalog No.
4. Title and Subtitle COMPUTER PROGRAM FOR CALCULATING FULL POTENTIAL TRANSONIC, QUASI-THREE-DIMENSIONAL FLOW THROUGH A ROTATING TURBOMACHINERY BLADE ROW		5. Report Date June 1982 6. Performing Organization Code 505-32-52
7. Author(s) Charles A. Farrell		8. Performing Organization Report No. E-1013
9. Performing Organization Name and Address National Aeronautics and Space Administration Lewis Research Center Cleveland, Ohio 44135		10. Work Unit No. 11. Contract or Grant No.
12. Sponsoring Agency Name and Address National Aeronautics and Space Administration Washington, D.C. 20546		13. Type of Report and Period Covered Technical Paper 14. Sponsoring Agency Code

15. Supplementary Notes

16. Abstract

A fast, reliable computer code is described for calculating the flow field about a cascade of arbitrary two-dimensional airfoils. The method approximates the three-dimensional flow in a turbomachinery blade row by correcting for stream-tube convergence and radius change in the throughflow direction. A fully conservative solution of the full potential equation is combined with the finite volume technique on a body-fitted periodic mesh, with an artificial density imposed in the transonic region to insure stability and the capture of shock waves. The instructions required to set up and use the code are included in this report. The name of the code is QSONIC. A numerical example is also given to illustrate the output of the program.

17. Key Words (Suggested by Author(s))	18. Distribution Statement
Potential flow Transonic Quasi-three-dimensional flow Rotating blade	Unclassified - unlimited STAR Category 02

19. Security Classif. (of this report)	20. Security Classif. (of this page)	21. No. of Pages	22. Price*
Unclassified	Unclassified	56	A04

* For sale by the National Technical Information Service, Springfield, Virginia 22161

NASA-Langley, 1982